

ADA 053324

6
REDUCTION OF OFFSHORE PLATFORM DYNAMIC RESPONSE BY
TUNED MASS DAMPER

by

10 ROBERT ALLAN GLACEL

R.S., United States Military Academy
(1969)

1
9 Master's thesis

Submitted in partial fulfillment
of the requirements for the
Degrees of

12 141p.

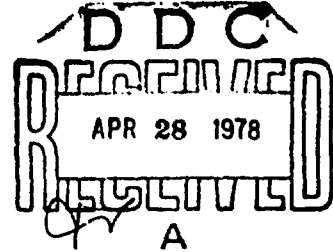
Master of Science in Mechanical Engineering

and

Master of Science in Civil Engineering

at the

Massachusetts Institute of Technology



11 May 1977

Signature of Author..... Robert Allan Glacel
Departments of Mechanical Engineering
and Civil Engineering, May 12, 1977

Certified by..... David N. Wonnley
Thesis Supervisor, Department of Mechanical Engineering

Certified by..... James J. Connor
Thesis Supervisor, Department of Civil Engineering

Accepted by.....
Chairman, Department of Mechanical Engineering Committee
on Graduate Students

Accepted by.....
Chairman, Department of Civil Engineering Committee
on Graduate Students

DISTRIBUTION STATEMENT A
Approved for public release;
Distribution Unlimited

220 000

AD NO. DDC FILE COPY

REDUCTION OF OFFSHORE PLATFORM DYNAMIC RESPONSE BY
TUNED MASS DAMPER

by

ROBERT ALLAN GLACEL

Submitted to the Department of Mechanical Engineering
and the Department of Civil Engineering on 12 May 1977
in partial fulfillment of the requirements for the Degrees
of Master of Science in Mechanical Engineering and Master
of Science in Civil Engineering

ABSTRACT

An investigation of a tuned mass damper for reduction of
offshore oil platform motions is conducted using finite element
tower models disturbed by discretized wave spectra.

Vibration control principles and their application to
offshore oil platforms are discussed.

Changes in system response are examined as damper parameters
are varied. Response reduction and damper mass motion are found to
be coequal design considerations.

An assessment is made of a tuned mass damper's effectiveness
in reducing the effects of increasing the natural period of
offshore platforms, fatigue in steel-jacketed platforms, and
soil-degradation under gravity platforms.

Thesis Supervisor:
Title:

David N. Wormley
Professor of Mechanical Engineering

Thesis Supervisor
Title:

Jerome J. Connor
Professor of Civil Engineering

ACCESSION NO.	
RTIC	<input checked="" type="checkbox"/>
DOC	<input type="checkbox"/>
CHAPTERS	<input type="checkbox"/>
JUSTIFIED	
<i>Letter on file</i>	
BY	
CUSTOMER'S AVAILABILITY CODES	
Dist.	Avail. or SPECIAL
A	

ACKNOWLEDGEMENTS

The author wishes to thank Professors David N. Wormley and Jerome J. Connor for their excellent and valuable guidance during the development of this thesis.

The author expresses his gratitude to Dr. Allen Marr for his invaluable contribution to the soil degradation analysis.

The author acknowledges with appreciation the computer time provided by the Departments of Mechanical Engineering and Civil Engineering at the ME-CE Joint Computer Facility.

Sincere appreciation is extended to Stephanie Demeris for the typing of this paper.

TABLE OF CONTENTS

	<u>Page</u>
TITLE PAGE	1
ABSTRACT	2
ACKNOWLEDGEMENTS	3
TABLE OF CONTENTS	4
LIST OF TABLES	6
LIST OF FIGURES	7
LIST OF SYMBOLS	9
CHAPTER 1 - INTRODUCTION	14
1.1 General Background	14
1.2 Scope of Thesis	17
CHAPTER 2 - THEORETICAL FORMULATIONS	19
2.1 The Structural Model	19
2.2 Hydrodynamic Forces	28
2.2.1 The Wave Amplitude Spectrum	28
2.2.2 Wave Forces of Offshore Platforms	34
2.3 Frequency Domain Solution	38
CHAPTER 3 - VIBRATION CONTROL SYSTEMS	40
3.1 The Dynamic Vibration Absorber Subject to Sinusoidal Input	40
3.2 The Damped Dynamic Vibration Absorber Subject to White Noise Input	46
3.3 The Mass Damper and the Offshore Platform	48
CHAPTER 4 - PARAMETER VARIATION AND SYSTEM RESPONSE	55
CHAPTER 5 - DAMPER APPLICATION TO INDUSTRY PROBLEMS	66
5.1 Offshore Platforms in Water Depths Greater than 1000 Feet	66

	<u>Page</u>
5.2 Fatigue Failure in Steel-Jacketed Platforms	69
5.3 Soil Degradation under Gravity Platforms	73
CHAPTER 6 - SUMMARY AND CONCLUSIONS	79
6.1 Summary of Findings	79
6.2 Conclusions	80
6.3 Areas for Further Study	80
REFERENCES	82
APPENDIX A - COMPUTER PROGRAM LISTING	84
APPENDIX B - MODEL MATRICES	114
APPENDIX C - MODAL ANALYSIS OF THE WAVE EXCITED PLATFORM	127
C.1 Natural Frequencies and Characteristic Shapes	127
C.2 Orthogonality of Modes	129
C.3 Modal Equations	130
C.4 Platform Analysis and Results	136

LIST OF TABLES

	<u>Page</u>
2.1 Model Finite Element Parameters	22
2.2 Damping Values for Various Materials	25
2.3 Variation of Computered Response with Damping	25
2.4 Natural Frequencies and Damping Parameters for Structural Models	27
2.5 Parameters for the P-M Wave Amplitude Spectrums Used in the Analysis	33
3.1 Mass Damper Parameters	53
4.1 Mass Damper Parameters for Minimum Response	64
5.1 Comparison of Tower Response when Subject to a 100 Year Return Sea State	67
5.2 Comparison of RMS Top Element Strain for 30 and 40 MPH Sea States	74
5.3 Comparison of Platform Response when Subject to 100 Year Return Sea State	78
C.1 Response Statistics of DOF 9(x_7) of 1000 Foot Tower	138

LIST OF FIGURES

	<u>Page</u>
2.1 Gravity and Steel-Jacketed Structure Models	20
2.2 Beam Element	29
2.3 Pierson-Moskowitz Wave Amplitude Spectra Used in the Analysis	32
2.4 Discretization of Typical Wave Amplitude Spectrum	35
2.5 Discretized Wave Spectra Used in the Analysis	36
3.1 One Degree of Freedom System Disturbed by Force $P \sin \omega t$	41
3.2 Main System M_1, K_1 with Vibration Absorber Attached	41
3.3 Response of One Degree of Freedom System to Disturbance $P \sin \omega t$ as a Function of ω	42
3.4 Response of Main System with Vibration Absorber Attached to Disturbance $P \sin \omega t$ as a Function of ω	42
3.5 Response Curves for Motion of the Main Mass	45
3.6 Crandall and Mark's Model Subject to White Noise Acceleration S_0	47
3.7 Deck Displacement vs. Frequency	50
3.8 Deck Acceleration vs. Frequency	51
3.9 Top Element Strain vs. Frequency	52
4.1 Displacement Ratios vs. Mass Ratio	57
4.2 Deck Displacement vs. Frequency (μ varying)	58
4.3 Displacement Ratios vs. Frequency Ratio	60

	<u>Page</u>
4.4 Deck Displacement vs. Frequency (ω_a/Ω_n varying)	61
4.5 Displacement Ratios vs. β_a	62
4.6 Deck Displacement vs. Frequency (β_a varying)	63
5.1 S-N Data in Salt Water Environment for Annealed Steel, 0.37% Carbon	71
5.2 Fundamental Period vs. Shear Modulus, Condeep	76

LIST OF SYMBOLS

A	Amplitude of free modal response
<u>B</u>	Vector relating nodal displacements to element strains
c_1	Damping coefficient of main system
c_2	Damping coefficient of absorber
c_c	Critical damping
c_D	Damping coefficient of damper in structural model
C_I	Inertial coefficient
<u>C_1</u>	Viscous damping matrix
<u>C_2</u>	Hysteretic damping matrix
d	Depth of beam element
D	Cylinder diameter
D_f	Damage fraction
$E[y_1^2]$	Expected value of the relative motion of main mass with vibration absorber attached
$E[\eta^2]$	Mean square of wave amplitudes
f	Cyclic frequency (Hz)
f_m	Frequency at which maximum occurs in wave spectrum
g	Forced frequency ratio (ω/Ω_n)
G	9.80 m/sec ²
h	Water depth from ocean floor to still water surface
H	Wave height from tip to trough

H_{\max}	Maximum wave height
H_s	Significant wave height
K	Wave number ($K = 2\pi/\lambda$)
k_1	Spring constant of main system
k_2	Spring constant of absorber
k_t	Stiffness of damper in structural model
k_L	Stiffness of translational soil springs
k_θ	Stiffness of rotational soil springs
\underline{K}	Stiffness matrix
\underline{K}_e	Equivalent stiffness matrix
L	Length of beam element
m_1	Mass of main system
m_2	Mass of absorber
m_D	Mass of damper in structural model
M	Number of DCF in structural model
\underline{M}	Mass matrix
\underline{M}_e	Equivalent mass matrix
N	Number of frequencies in discretized spectrum
N_f	Number of cycles of loading to failure
p	Ratio of damping to critical damping (c/c_c)
P	Force
\underline{P}	Vector of forces

$P(\omega_i)$	Force vector at frequency ω_i
r	Natural frequency ratio (ω_a/Ω_n)
S	Stress
S_o	White noise acceleration
$S_{\eta\eta}(\omega)$	Wave amplitude spectrum
T_f	Time to failure
T_1, T_2	First two natural periods of a structure
\dot{u}	Fluid particle acceleration
U	Windspeed reported by Weatherships
\underline{u}	Vector of modal amplitudes
$\underline{\ddot{u}}$	Vector of modal accelerations
x_o	Base displacement
x_1	Displacement of mass of main system in 1 or 2-DOF model
x_2	Displacement of mass of absorber in 2-DOF model
x_D	Displacement of damper mass in structural model
x_i	Displacement of DOFi in structural model
\dot{x}_1	Velocity of mass of main system in 1 or 2-DOF model
\dot{x}_2	Velocity of mass of absorber in 2-DOF model
\ddot{x}_1	Acceleration of mass of main system in 1 or 2-DOF model
\ddot{x}_2	Acceleration of mass of absorber in 2-DOF model
X_{st}	Static deflection of main system
X_1	Steady state amplitude of main system dynamic response
X_2	Steady state amplitude of absorber dynamic response

\underline{x}	Vector of displacements
$\underline{\dot{x}}$	Vector of velocities
$\underline{\ddot{x}}$	Vector of accelerations
$\underline{x}(\omega_i)$	Displacement vector at frequency ω_i
$\underline{\ddot{x}}(\omega_i)$	Acceleration vector at frequency ω_i
\underline{X}_n	Vector of modal displacements for nth mode
y_1	Relative displacement of main mass ($y_1 = x_1 - x_0$)
z	Distance from ocean floor to any elevation on a structure
α	$4\pi \left[\frac{\lambda_1}{T_2} - \frac{\lambda_2}{T_1} \right] / \left[\frac{T_1}{T_2} - \frac{T_2}{T_1} \right]$
α_s	8.10×10^{-3}
β	0.74
β_a	Percent critical damping in mass damper
β_H	Percent critical hysteretic damping
β_n	Percent critical damping in structural model
β_v	$\frac{1}{\pi} [\lambda_2 T_1 - T_2 \lambda_1] / \left[\frac{T_1}{T_2} - \frac{T_2}{T_1} \right]$
Δ	Increment of frequency
ϵ	Element strain
$\epsilon(\omega_i)$	Element strain at frequency ω_i
η	Wave amplitude
$\eta(\omega_i)$	Discretized wave amplitude at frequency ω_i
θ_i	Rotation of DOFi in structural model
λ	Wavelength
λ_1, λ_2	Percent critical viscous damping assumed in the first two structural modes

μ	Mass ratio (m_2/m_1)
ρ	Density of fluid
σ_x^2	Mean square displacement
$\sigma_{\ddot{x}}^2$	Mean square acceleration
σ_y^2	Expected value of the motion of the main mass without the vibration absorber
σ_ϵ^2	Mean square element strain
σ_η^2	Variance of wave amplitudes
$\frac{\sigma_D}{\sigma}$	Deck displacement ratio
$\frac{\sigma_{\text{damper}}}{\sigma}$	Ratio of RMS relative damper displacement to the RMS deck displacement without the mass damper
ϕ_I	Inertial force per unit of cylinder length
ϕ_T	Total force per unit of cylinder length
$\phi_T(\omega_i)$	Total force per unit of cylinder length at frequency ω_i
$\underline{\phi}$	Modal matrix
ω	Circular frequency (rad/sec)
ω_a	Natural frequency of absorber
ω_o	G/U
Ω_1, Ω_n	Natural frequency of main system/Fundamental frequency of the structural model
Ω_2	Second natural frequency of structural model

CHAPTER 1

INTRODUCTION

1.1 General Background

Because the search for oil is becoming more intense, as the need for petroleum products grows, the oil industry is exploring offshore areas where the environment is hostile. To overcome the elements and still produce oil, the industry has adopted new platform concepts. In the North Sea, large concrete structures called gravity platforms are in use. These platforms rest on the ocean floor in 550 feet of water relying only on their own weight to keep them stable in one of the roughest ocean environments in the world. In the Gulf of California and the Gulf of Mexico, steel jacketed platforms are being constructed to bring oil from deep water. Exxon's platform is placed in 850 feet of water off the Coast of California and Shell's platform will operate in 1000 feet of water in the Gulf of Mexico.

As is usual when new concepts are employed in extreme conditions, problems have developed which demand consideration. A survey of industry people involved in the implementation of these new concepts and a review of current literature addressing these concepts reveals three problems of major concern to the industry with regard to offshore platforms.

The first problem is designing a platform for use in water deeper than 1000 feet and still having the design remain economical. Industry sources reveal that a general rule of thumb developed from experience

limits the fundamental period of offshore platforms to a maximum of five seconds. This results from the fact that the waves with the greatest energy content have frequencies greater than five seconds. Limiting the fundamental period of the structure to five seconds or less minimizes the dynamic effects of the wave loads on the structure in the frequency range of waves which produce the largest forces, thus reducing the ultimate load on the structure. If a platform is designed without reinforcement for use in water of depths greater than 1000 feet, the fundamental period is greater than five seconds resulting in a higher ultimate load on the structure and requiring more structural material adding to the cost. If a platform is designed with reinforcement so that the fundamental period is five seconds or less for water depths greater than 1000 feet, the ultimate load on the structure is reduced, but the cost of the reinforcing material is high.

The second problem is combating the low cycle - high stress fatigue of deep water steel jacketed structures in severe ocean environments such as the North Sea. Nearly all industry sources surveyed agreed that dynamically amplified fatigue becomes a major consideration in design as steel jacketed platforms [with fundamental periods greater than four seconds] move into deeper water in areas such as the North Sea. Here, conditions are such that normal day-to-day waves with frequencies near the fundamental frequency of the structure contain sufficient energy to reduce significantly the life expectancy of the structure through fatigue failure. Kallaby

and Price [1] calculated the cost of overcoming fatigue effects in these structures and found that the fatigue premium was 4.5% of the cost of the structure.

The third problem concerns degradation of the soil under gravity platforms due to cyclic loading during storm conditions. As large waves strike the gravity structure, forces are transmitted to the soil in the form of stress increases or decreases between the soil and the structure. The nature of wave loading causes these stress changes to be cyclic. Increased stresses in the soil cause increases in the pore-water pressure of the soil and cyclic stress reversals cause the pore-water pressure to increase with time. As the pore pressure increases, the soil becomes weaker and finally loses all strength through liquefaction. Calculations on soil degradation resulting from this type of loading have been done by Bjerrum [2], Anderson [3] and Hoeg [4]. They show that over a period of storms it is possible for the strength of soil beneath a gravity platform such as those in operation in the North Sea to be reduced significantly. Tayloe [5], Watt et al [6] and Utt et al [7] showed that as the soil strength degraded in the fashion described above, the weakened foundation caused the fundamental period of the structure to increase into the range where dynamic amplification of the peak load would occur, thereby increasing the ultimate load on the structure perhaps beyond the design load. The offshore industry has no field data available at this time to assess the seriousness of this problem but steps are being taken to secure an answer in the next few years.

It has been suggested that an effective and economic means of overcoming some of the problems described above is the use of a mass damper on structures used in deep water. The mass damper is an energy absorbing system consisting of a mass-spring-dashpot apparatus placed near the deck of deep water platforms which, when properly tuned, reduces the dynamic response of the platform. The mass damper is not a new concept. In its earliest and simplest form it was known as a vibration absorber and was used in industry applications to reduce vibrations [8]. Recently, however, the mass damper has been installed in two tall buildings to reduce their response to wind inputs. The extension of the mass damper concept to offshore platforms and the effectiveness of such a system in overcoming the problems cited above is the subject of this thesis.

1.2 Scope of Thesis

To examine the potential use of a mass damper on an offshore platform, this thesis addresses two questions: how effective is the system when used on a multi-degree of freedom offshore tower subject to frequency dependent sea states and how does system response change as damper parameters are varied?

To pursue these answers, offshore platforms are modelled with a finite element computer program developed by DuVall [9] which computes the frequency domain response of an offshore platform to designated sea states. The platform models are of two types: steel-jacketed structures with fundamental periods ranging from

5-7 seconds and a concrete gravity platform of the Condeep type with a fundamental period of about three seconds. The various sea states used as environmental input are modeled by the Pierson-Moskowitz wave amplitude spectrum which is developed in Chapter 2. DuVall's program has been modified to include the mass damper, structural damping, and soil effects.

The vibration absorber and mass damper are explained and their mathematics discussed.

An illustrative analysis is presented showing structural responses with and without the mass damper in operation. Next, a modal analysis of this same example is made to determine participation of each mode in the total structural response.

Finally the multi-modal model platform is analyzed for varying sea states to determine damper effectiveness and the variation of system response with damper parameters. Results are presented and discussed and an evaluation of overall effectiveness and feasibility is made.

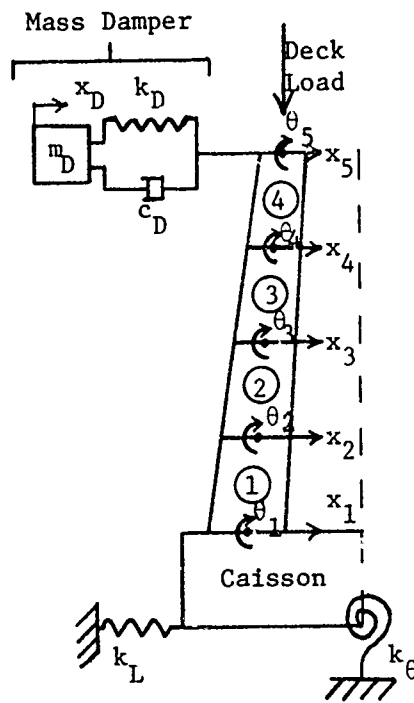
CHAPTER 2
THEORETICAL FORMULATIONS

2.1 The Structural Model

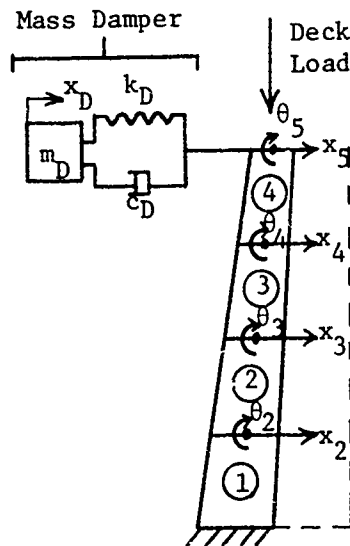
The offshore platforms analyzed in this thesis are modelled using a finite element computer program developed by DuVall [9]. This program assembles a model of an offshore platform, either gravity or steel-jacketed, based on platform dimensions input by the user. Both types of structures are modelled (see Figure 2.1) as 4 two-dimensional axisymmetric beam elements supporting a load representing the deck.

The gravity structure model supports the beam elements with a caisson which rests on a flexible soil base represented by linear springs. This model has ten degrees of freedom when the mass damper is not in operation. These are x_1 through x_5 and θ_1 through θ_5 as shown in Figure 2.1. When the mass damper is in operation, an additional degree of freedom, x_D , is added bringing the total to eleven.

The steel-jacketed model fixes the beam elements to the ocean floor in a cantilever fashion representative of piled structures. This model has eight degrees of freedom when the mass damper is not in operation. Degrees of freedom x_1 and θ_1 are set to zero as boundary conditions representing a fixed base and the remaining degrees of freedom are x_2 through x_5 and θ_2 through θ_5 . An additional degree of freedom, x_D , is added when the mass damper is in operation.



Gravity Structure Model



Steel-Jacketed Structure Model

Figure 2.1

The models are loaded in their plane using a discretized wave height spectrum (see Section 2.2.1) and the model response is given as discretized frequency spectrums of horizontal displacements and accelerations, and in-plane rotations of the beam element nodes. It has been shown by Nath [10] that platform response is independent of the direction of loading so that a two-dimensional model is valid for analysis.

Three models are used in the subsequent analysis: the 1000 foot steel-jacketed platform currently being constructed by Shell Oil Corporation, a 1200 foot steel-jacketed platform of theoretical design, and the Condeep Brent B gravity platform in operation in the North Sea. Table 2.1 lists the finite element model parameters for each model.

DuVall's program has been modified to include damping effects and a mass damper in the analysis, and the output of a discretized frequency spectrum of element strains. A detailed description of the unmodified program can be found in [9]. Appendix A contains a listing of the modified program.

Two types of damping, viscous and hysteretic, are incorporated into the program. Viscous damping accounts for fluid-structure interaction and slippage and rubbing in structural joints. It is assumed to be linearly proportional to the structure's velocity and is represented by the matrix \underline{C}_1 in the equation of motion:

$$\underline{M} \ddot{\underline{x}} + \underline{C}_1 \dot{\underline{x}} + \underline{Kx} = \underline{P} \quad (2.1)$$

	1000 Ft. Steel-Jacket	1200 Ft. Steel-Jacket	Condeep Gravity
Height	366 m	427 m	173 m
Water Depth	305 m	366 m	145 m
External Radius			
Base	33.75 m	37.875 m	17.3 m
Platform	9.0 m	9.0 m	4.9 m
Internal Radius			
Base	33.6 m	37.717 m	16.0 m
Platform	8.9 m	8.9 m	4.75 m
Deck Mass	4180.0 MT-sec ² /m	7500.0 MT-sec ² /m	1580.0 MT-sec ² /m
Deck Inertia	2432760 MT-sec ² /m	2432760 MT-sec ² /m	500187 MT-sec ² /m
Total Mass	11213.0 MT-sec ² /m	22304.0 MT-sec ² /m	17141.0 MT-sec ² /m
Modulus of Elasticity	2.039 x 10 ⁷ MT/m ²	2.039 x 10 ⁷ MT/m ²	2.9 x 10 ⁶ MT/m ²
Caisson Height	-	-	60.0 m
Caisson Radius	-	-	39.7 m
Caisson Mass	-	-	15330.0 MT-sec ² /m ²
Soil Density	-	-	400.0 MT-sec ² /m ⁴
Shear Modulus	-	-	5000.0 MT/m ²
v Soil	-	-	.5

Table 2.1
Model Finite Element Parameters

where

\underline{M} = mass matrix

\underline{K} = stiffness matrix

\underline{P} = vector of forces

$\ddot{\underline{x}}$ = vector of accelerations

$\dot{\underline{x}}$ = vector of velocities

\underline{x} = vector of displacements

Determining the proper viscous damping for multi-degree of freedom systems is difficult because the nature of damping is not well described. In terms of the idealized model there is no "exact" way to assign values to the elements of \underline{C}_1 . One method, described by Maddox [11], and used in this analysis, assumes Rayleigh type damping which corresponds to

$$\underline{C}_1 = \alpha \underline{M} + \beta_v \underline{K} \quad (2.2)$$

where α and β_v are scalars defined by:

$$\alpha = 4\pi \left[\frac{\lambda_1}{T_2} - \frac{\lambda_2}{T_1} \right] / \left[\frac{T_1}{T_2} - \frac{T_2}{T_1} \right] \quad (2.3)$$

$$\beta_v = \frac{1}{\pi} [\lambda_2 T_1 - T_2 \lambda_1] / \left[\frac{T_1}{T_2} - \frac{T_2}{T_1} \right]$$

and

λ_1, λ_2 = percent critical damping assumed in the first two structural modes

T_1, T_2 = first two natural periods of the structure.

With only viscous damping considered the equation of motion becomes:

$$\underline{M} \ddot{\underline{x}} + (\alpha \underline{M} + \beta_v \underline{K}) \dot{\underline{x}} + \underline{K} \underline{x} = \underline{P} \quad (2.4)$$

Hysteretic damping is due to internal friction within the material itself and is proportional to the stiffness and the deflection of the structure. It is modelled as:

$$\underline{C}_2 = 12\beta_H \underline{K} \quad (2.5)$$

where

$$i = \sqrt{-1}$$

β_H = percent critical hysteretic damping

Including hysteretic damping, the equation of motion becomes

$$\underline{M} \ddot{\underline{x}} + (1 + 12\beta_H) \underline{K} \underline{x} = \underline{P} \quad (2.6)$$

When both viscous and hysteretic damping effects are considered the equation of motion for the structure expands to

$$\underline{M} \ddot{\underline{x}} + (\alpha \underline{M} + \beta_v \underline{K}) \dot{\underline{x}} + (1 + 12\beta_H) \underline{K} \underline{x} = \underline{P} \quad (2.7)$$

There is general agreement on the representation of damping in a structure but no agreement has been reached concerning values for λ_1 , λ_2 , and β_H . A survey of several authors indicates that overall damping in offshore structures can vary from 1% of critical to 5% of critical damping depending on the author and type of structure. In general, most values ranged around 3%. Table 2.2 shows values of percent critical damping for different materials estimated by Zijp et al [12]. Note that a steel structure in water combines a 1% critical damping value for steel and a 1.5%

Material	Damping (% of Critical)
Soil, Translation	9
Soil, Rocking	4
Steel	1
Concrete	2
Hydrodynamic	1.5

Table 2.2
Damping Values for Various Materials [11]

Percent Critical Damping A	Standard Deviation of Response at A% Critical Damping
	Standard Deviation of Response at 3% Critical Damping
1	1.7
3	1.0
5	0.8

Table 2.3
Variation of Computed Response with Damping

critical damping value for hydrodynamic effects to display 2.5% critical damping overall. Similarly, a concrete structure in water displays 3.5% critical damping overall. Again the values range around 3%.

A concern in choosing a value of overall damping is the sensitivity of the structural response to that value. To check the sensitivity of the model to changes in overall damping, the response of the 1000 foot model to wave excitation was calculated for different values of overall damping. Results of these computations, shown in Table 2.3, indicate that the response is very sensitive to damping. Table 2.3 shows that as damping is decreased from 3% to 1% of critical, the response standard deviation increases by a factor of 1.7. As the damping is increased to 5% of critical, the response decreases to 0.8 of the 3% response. Therefore as damping is increased, the rate of change of the response is reduced, but in the range of damping found in offshore structures, the change in response can be significant for small changes in structural damping.

Because the value of damping in any structure can only be estimated and the response is dependent on the value chosen, a difficult situation arises. This analysis uses the damping value most often found in research, 3% critical damping for all cases, with viscous and hysteretic damping each accounting for one-half the damping. Therefore, $\lambda_1 = \lambda_2 = \beta_H = 1.5\%$ of critical damping. Table 2.4 shows the values of the damping parameters α , β_v and β_H

		1000 ft Steel-Jacket	1200 ft Steel-Jacket	Condeep Gravity
First Natural Frequency	Ω_1	1.244 rad/sec	.905 rad/sec	2.094 rad/sec
Second Natural Frequency	Ω_2	5.712 rad/sec	4.217 rad/sec	4.189 rad/sec
First Natural Period	$T_1 = \frac{2\pi}{\Omega_1}$	5.05 sec	6.94 sec	3.00 sec
Second Natural Period	$T_2 = \frac{2\pi}{\Omega_2}$	1.10 sec	1.49 sec	1.50 sec
	λ_1	.015	.015	.015
	λ_2	.015	.015	.015
	α	.0302	.0224	.0420
	β_v	.0043	.0059	.0048
	β_H	.015	.015	.015

Table 2.4

Natural Frequencies and Damping Parameters for Structural Models

for the three models to be used in this study.

The mass damper is modelled as a simple spring-mass-dashpot system connected to the top node of the structure (see Figure 2.1).

Computation of element strains have been included in the modified program. For the beam element used in this program and displayed in Figure 2.2, the strain at any point in the element equals:

$$\begin{aligned} \epsilon = & \left[-x \left(-\frac{6}{L^2} + \frac{12y}{L^3} \right) \right] x_1 + \left[-x \left(-\frac{4}{L} + \frac{6y}{L^2} \right) \right] \theta_1 \\ & + \left[-x \left(\frac{6}{L^2} - \frac{12y}{L^3} \right) \right] x_2 + \left[-x \left(\frac{2}{L} + \frac{6y}{L^2} \right) \right] \theta_2 \end{aligned} \quad (2.8)$$

Midpoint strains are taken as the representative strain measures for the elements. Specializing (2.8) results in

$$\epsilon = \frac{d}{2L} [\theta_1 - \theta_2] \quad (2.9)$$

2.2 Hydrodynamic Forces

2.2.1 The Wave Amplitude Spectrum

Common models for the surface of the sea assume the water surface can be described as a stationary, ergodic Gaussian, or normal process with zero mean [13].

A stationary process is one for which the statistics of the process, or the probability law, remain constant with respect to time. An ergodic process is one in which any averages taken with respect to a fixed position, with respect to time, are equal to

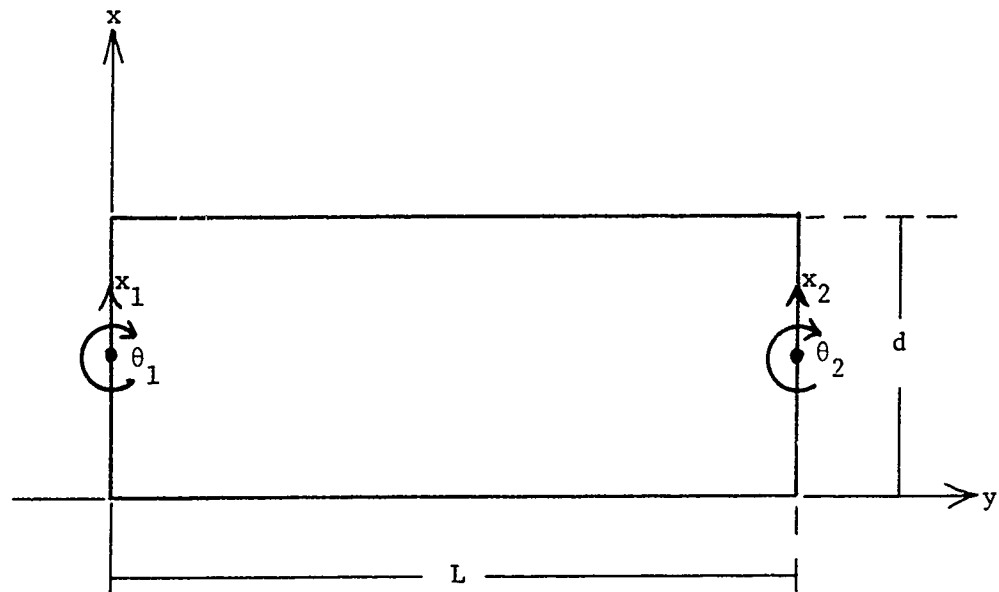


Figure 2.2
BEAM ELEMENT

averages taken at a fixed time over the ensemble, or collection, of all possible realizations of the process.

Because of these properties, the sea at any place and time can be described as a wave amplitude spectrum, $S_{\eta\eta}(\omega)$ which has the property that the variance of the wave amplitudes is equal to the integral of the wave amplitude spectrum over all positive frequencies, or

$$\sigma_{\eta}^2 = E(\eta^2) = 2 \int_0^{\infty} S_{\eta\eta}(\omega) d\omega \quad (2.10)$$

where

$S_{\eta\eta}(\omega)$ = wave amplitude spectrum in m^2/sec

σ_{η}^2 = variance of wave amplitudes (in spectrum)

$E(\eta^2)$ = mean square of wave amplitudes (in spectrum)

η = wave amplitude associated with random ocean wave

Of the several empirically derived wave amplitude spectra available, the most widely used is the Pierson-Moskowitz spectrum [14] representing a fully developed sea. Its form is

$$S_{\eta\eta}(\omega) = \left(\frac{\alpha_s G^2}{\omega^5}\right) e^{-\beta \left(\frac{\omega}{\omega_0}\right)^4} \quad (2.11)$$

where

$$\alpha_s = 8.10 \times 10^{-3}$$

$$\beta = 0.74$$

$$G = 9.80 \text{ m/sec}^2$$

$$\omega_0 = G/U$$

U = windspeed reported by weatherships in m/sec

Any one of four parameters can be used to specify a specific sea state. These are U , f_m , H_s , and H_{max} where

$$f_n = \frac{\omega_0}{2\pi} = \frac{G}{2\pi U}$$

$$H_s = 4\sqrt{\int_0^{\infty} S\eta\eta(\omega) d\omega} = 4.078 \times 10^{-3} \left(\frac{G}{f_m^2}\right)$$

$$H_{max} = 2H_s$$

In this analysis, three specific Pierson-Moskowitz wave amplitude spectrums are used. They correspond to seas generated by 70 mph winds, 40 mph winds and 30 mph winds and are plotted in Figure 2.3. Table 2.5 contains the parameters of these seas. A detailed development of random waves and the wave spectrum can be found in Nath [10].

The computer program of DuVall uses a condensed spectrum represented by a finite number of frequencies. This condensed spectrum is derived by evaluating the area between $\omega-\Delta$ and $\omega+\Delta$ of the P-M spectrum around a specified frequency ω , taking the square root of that area, and assigning that value to the specific frequency. This is the rms wave amplitude in the band $\omega-\Delta$ to $\omega+\Delta$. This is done for all the frequencies specified, forming a histogram of frequencies and equivalent wave amplitudes which represent the P-M spectrum, from $\omega = 0$ to $\omega = .35$ rad/sec. Although the actual spectrum does not equal zero until $\omega = \infty$, the area under the spectrum

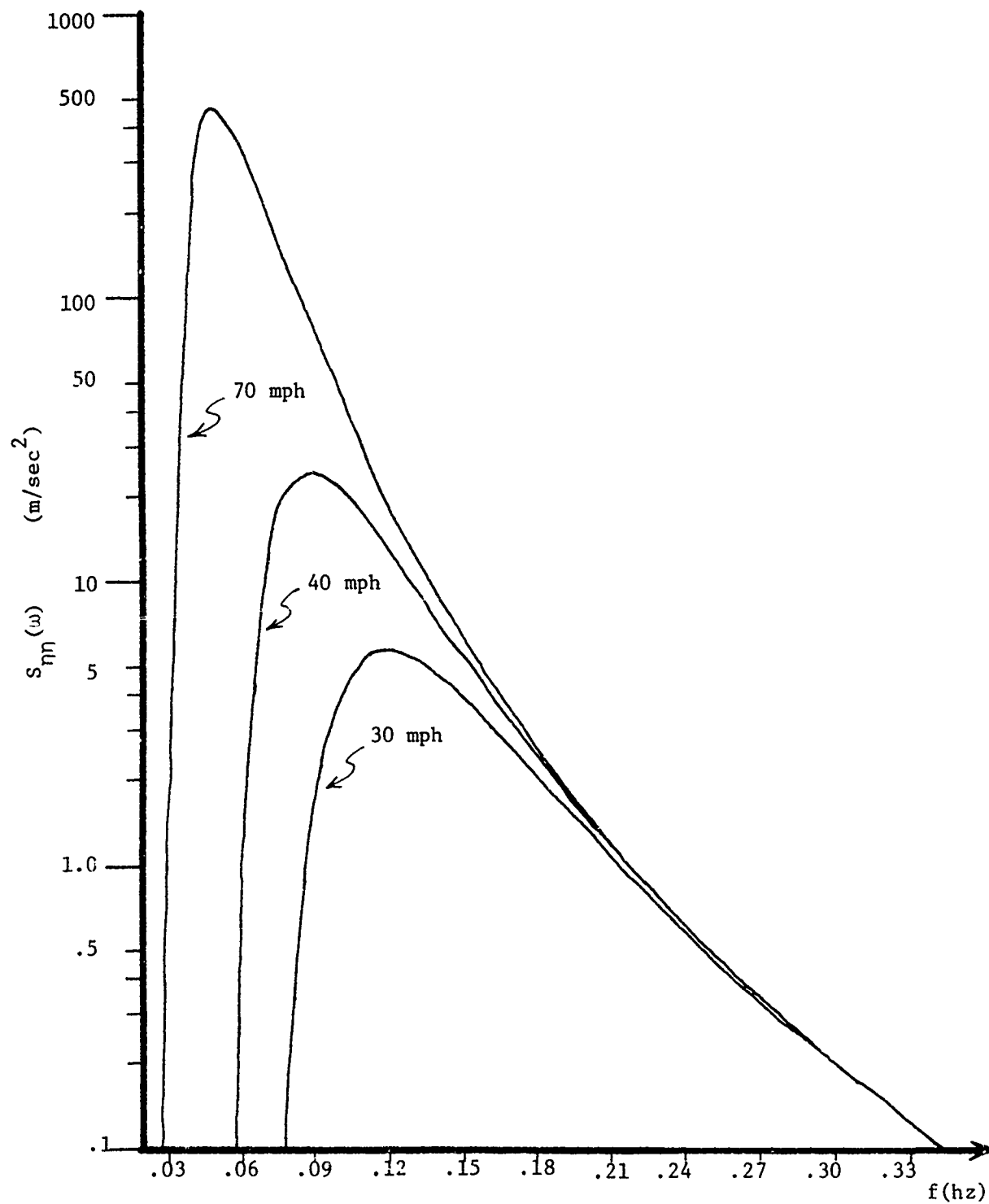


Figure 2.3

Pierson-Moskowitz Wave Amplitude Spectra Used in the Analysis

Windspeed	70 MPH	40 MPH	30 MPH
f_m	.05 hz	.09 hz	.12 hz
H_s	52.5 ft/16.0 m	16.2 ft/4.9 m	9.0 ft/2.7 m
H_{max}	105.0 ft/32.0 m	32.4 ft/9.8 m	18.0 ft/5.4 m

Table 2.5

Parameters for the P-M Wave Amplitude Spectrums
Used in the Analysis

from $\omega = .35$ to $\omega = \infty$ is only .05% of the total area from $\omega = 0$ to $\omega = \infty$, which is insignificant. An example of this process and the resulting discretized wave amplitude spectrum $\eta(\omega_i)$ is shown in Figure 2.4. The discretized wave amplitude spectrum for the three sea states used in this analysis are shown in Figure 2.5.

The discretized spectrum has the property that the variance of the wave amplitudes represented by the wave-amplitude spectrum is equal to the sum of the squares of the discretized wave amplitudes, that is

$$\sigma_{\eta}^2 = \sum_{i=1}^N (\eta(\omega_i))^2 \quad (2.12)$$

2.2.2 Wave Forces on Offshore Platforms

An expression for the total wave force on a cylinder per unit of cylinder length has been developed by Morison (1950). This total force consists of two parts, a drag component and an inertial component. The drag component can be shown to be negligible for deep water structures. Therefore the total force per unit of cylinder length is assumed here to consist of only the inertial component which is expressed as

$$\Phi_T = \Phi_I = \rho C_I \frac{\pi D^2}{4} \dot{u} \quad (2.13)$$

where

Φ_T = total force per unit of cylinder length

Φ_I = inertial force per unit length

ρ = density of fluid transmitting the wave

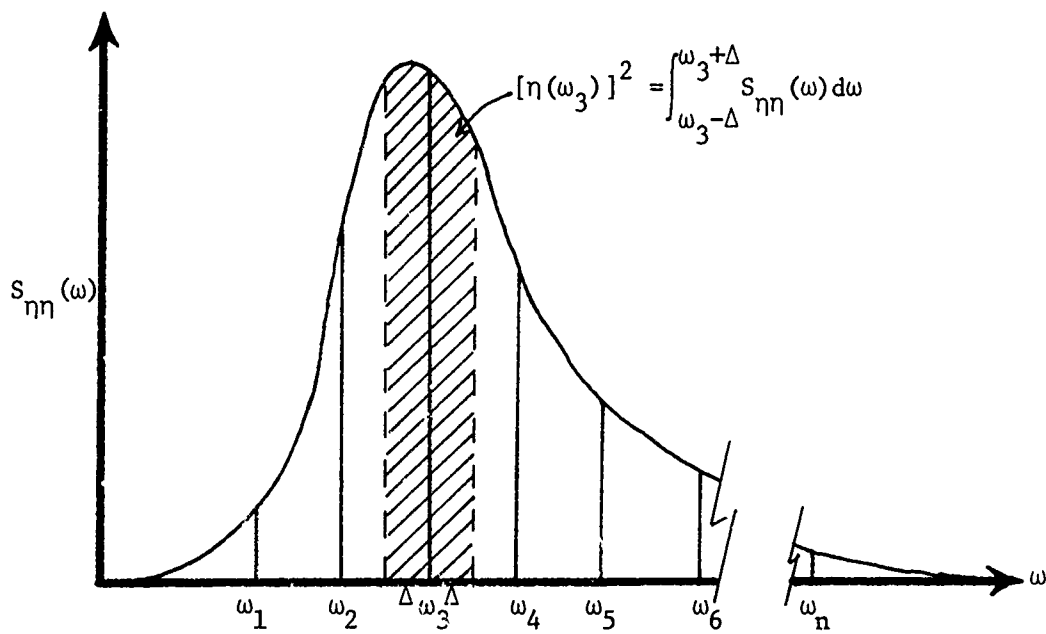


Figure 2.4a
Typical Wave Amplitude Spectrum

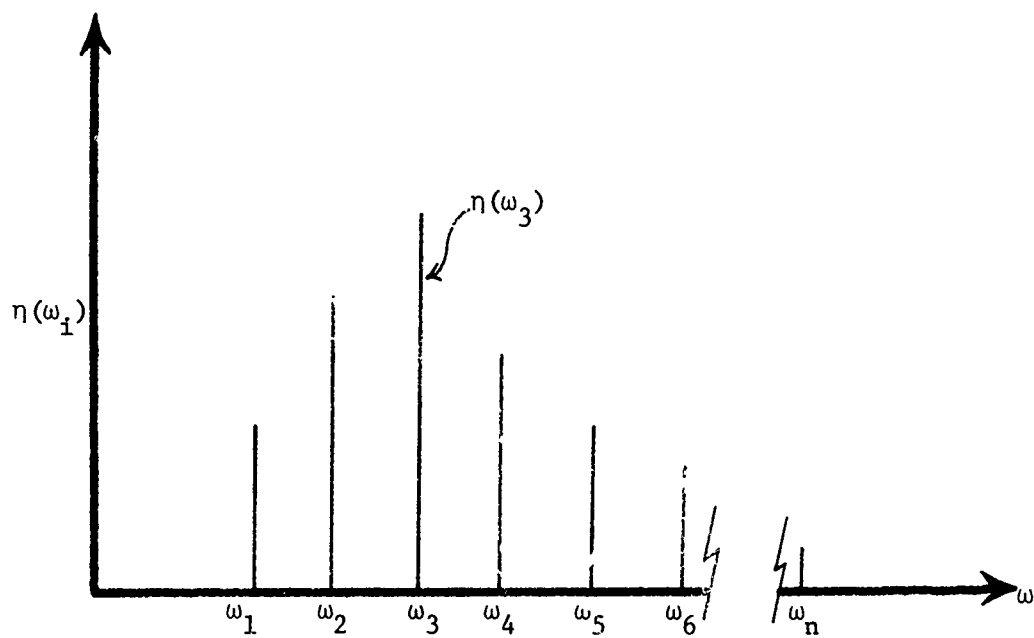


Figure 2.4b
Discretized Wave Amplitude Spectrum

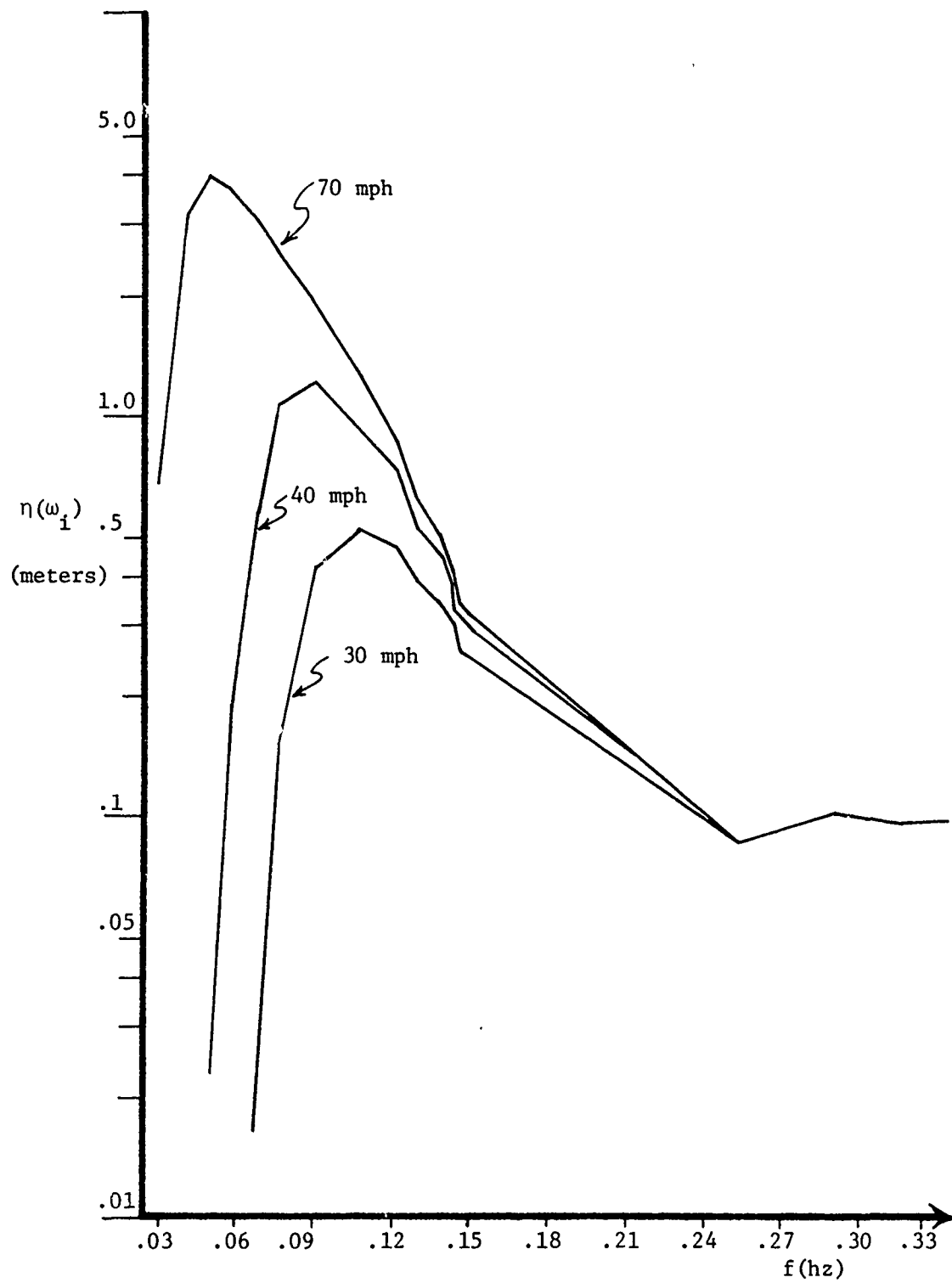


Figure 2.5

Discretized Wave Spectra Used in the Analysis (49 Frequencies)

C_I = inertial coefficient

D = cylinder diameter

\dot{u} = fluid partical acceleration

Airy wave theory shows that

$$\dot{u} = \frac{H}{2} \omega^2 \frac{\cosh(Kz)}{\sinh(Kh)} \sin\omega t \quad (2.14)$$

where

H = wave height from tip to trough

K = wave number, $K = 2\pi/\lambda$

λ = wave length

h = water depth from ocean floor to still water surface

z = distance from ocean floor to any elevation on
structure

$$\omega^2 = KG \tanh(Kh)$$

Therefore

$$\Phi_T = \frac{H}{2} \rho C_I \omega^2 \frac{\pi D^2}{4} \frac{\cosh(Kz)}{\sinh(Kh)} \sin\omega t \quad (2.15)$$

Since a single wave is described by $\eta = \frac{H}{2} \sin\omega t$, a linear relationship with respect to amplitudes exists between η and Φ_T .

This linear relationship allows the use of the discretized wave amplitude spectrum so that

$$\Phi_T(\omega_1) = (TF)\eta(\omega_1) \quad (2.16)$$

where

$$TF = C_I \rho \frac{\pi D^2}{4} \omega^2 \frac{\cosh(Kz)}{\sinh(Kh)} \quad (2.17)$$

A detailed development of this subject can be found in Nath [10].

Using the set of force distributions $\Phi_T(\omega_i)$ where $i = 1, N$, the computer program determines a vector of work-equivalent nodal forces \underline{P} for each ω_i to be applied to the structure during the frequency domain analysis. Development of this procedure is covered by DuVall [9].

2.3 Frequency Domain Solution

Using the set of vectors $\underline{P}(\omega_i)$ determined from the set of force distributions $\Phi_T(\omega_i)$ in Section 2.2.2 to excite the structural model, the displacement response is found by the computer program to be a set of vectors $\underline{x}(\omega_i)$ such that

$$\underline{x}(\omega_i) = (\underline{TF}) \underline{P}(\omega_i) \quad (2.18)$$

The model is represented by a linear system whose equation of motion is

$$\underline{M} \ddot{\underline{x}} + (\alpha \underline{M} + \beta \underline{K}_v) \dot{\underline{x}} + (1 + i2\beta_H) \underline{K} \underline{x} = \underline{P} \quad (2.7)$$

Assuming $\underline{P} = \underline{P}(\omega)e^{i\omega t}$ and $\underline{x} = (\underline{TF}) \underline{P}(\omega)e^{i\omega t}$, substituting into the equation of motion yields

$$(-\omega^2 \underline{M} + i\alpha\omega \underline{M} + \underline{K} + i2\beta_H \underline{K} + i\omega\beta \underline{K}_v) (\underline{TF}) \underline{P}(\omega)e^{i\omega t} = \underline{P}(\omega)e^{i\omega t} \quad (2.19)$$

It follows that

$$\underline{TF} = (-\omega^2 \underline{M} + i\alpha\omega \underline{M} + \underline{K} + i2\beta_H \underline{K} + i\omega\beta \underline{K}_v)^{-1} \quad (2.20)$$

The linearity of the system allows the transfer of the properties of the input to the response so that the variance of the response of

each degree of freedom is equal to the sum of the squares of responses of that degree of freedom at each discretized frequency.

$$(\sigma_x^2)_j = \sum_{i=1}^N (x(\omega_i)_j)^2 \quad j=1, M \quad (2.21)$$

where M = number of degrees of freedom in the model.

To determine acceleration response, the following is used:

$$\ddot{x}(\omega_i) = -\omega_i^2 x(\omega_i) \quad (2.22)$$

and

$$(\sigma_{\ddot{x}}^2)_j = \sum_{i=1}^N (\ddot{x}(\omega_i)_j)^2 \quad j=1, M$$

Element strains are computed using the relationship

$$\varepsilon(\omega_i)_K = B_K [x(\omega_i)]_K \quad K = 1, 4 \quad (2.23)$$

where, as outlined in Section 2.1,

$$B_K = [0, (\frac{d}{2L})_K, 0, (\frac{d}{2L})_K]$$

$$[x(\omega_i)]_K^T = [x_1(\omega_i)_K, \theta_1(\omega_i)_K, x_2(\omega_i)_K, \theta_2(\omega_i)_K]$$

K = element number

and finally the variance of each element strain is found to be

$$(\sigma_\varepsilon^2)_K = \sum_{i=1}^N (\varepsilon(\omega_i)_K)^2 \quad (2.24)$$

CHAPTER 3

VIBRATION CONTROL SYSTEMS

3.1 The Dynamic Vibration Absorber Subject to Sinusoidal Input

The undamped dynamic vibration absorber, invented by Frahm in 1909, is used to eliminate unwanted vibrations from machinery.

Consider a machine represented by a one degree of freedom system subject to an unwanted sinusoidal force $P\sin\omega t$ (Figure 3.1).

Let the vibration absorber be represented by a comparatively small vibratory system k_2, m_2 , attached to the main mass m_1 (Figure 3.2).

If the parameters k_2, m_2 are chosen so that the natural frequency $(k_2/m_2)^{1/2}$ of the attached absorber is equal to the frequency ω of the disturbing force, then the main mass m_1 will not vibrate at all. The mathematical proof of this is contained in DenHartog [8].

This result is most useful when the frequency of the disturbing force is near the natural frequency of the main system putting that system at or near resonance. Consider the case where the main system whose response spectrum is shown in Figure 3.3, is disturbed at its natural frequency. A vibration absorber is added whose natural frequency equals the disturbing frequency which equals the natural frequency of the main system, or:

$$\omega_a = \Omega_n \text{ or } \frac{k_2}{m_2} = \frac{k_1}{m_1} \text{ or } \frac{k_2}{K_1} = \frac{m_2}{m_1} = \mu$$

where

$$\omega_a = (k_2/m_2)^{1/2} = \text{natural frequency of absorber}$$

$$\Omega_n = (k_1/m_1)^{1/2} = \text{natural frequency of main system}$$

$$\mu = m_2/m_1 = \text{mass ratio} = \text{absorber mass/main mass}$$

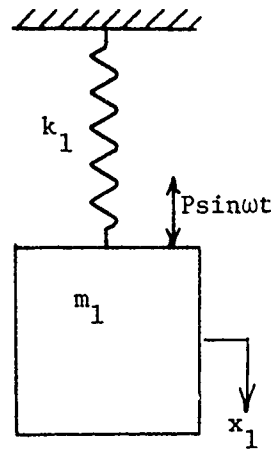


Figure 3.1

One Degree of Freedom System Disturbed by Force $P \sin \omega t$

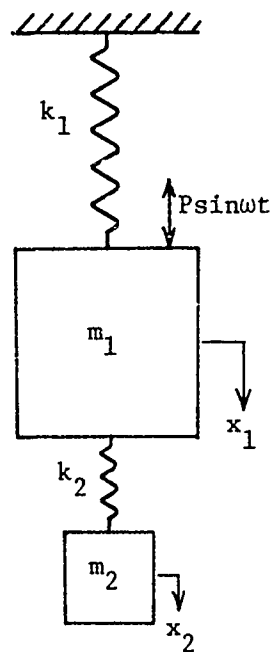


Figure 3.2

Main System m_1, k_1 with Vibration Absorber Attached

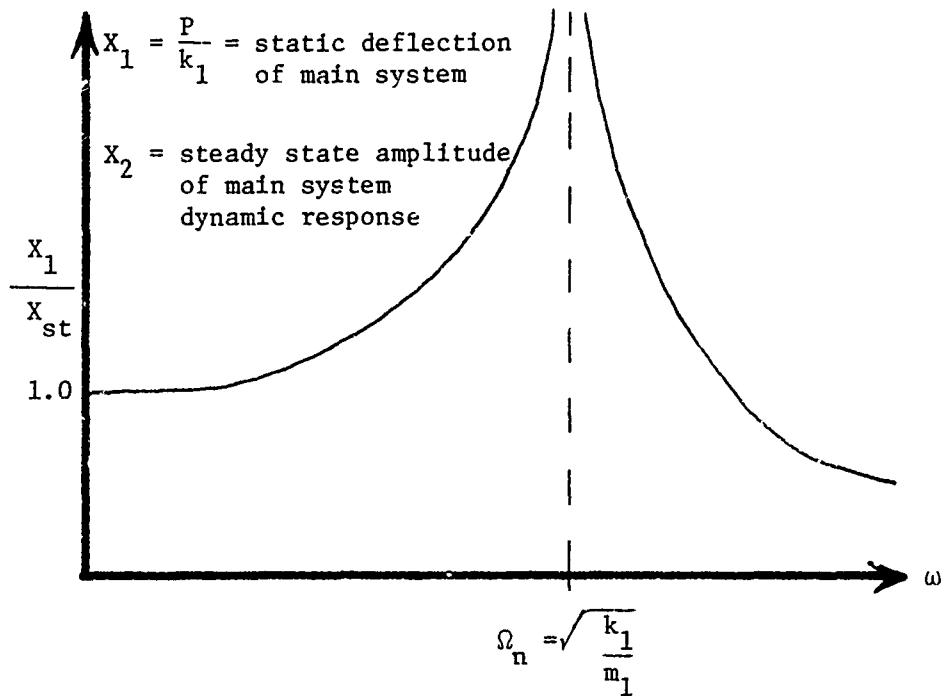


Figure 3.3

Response of One Degree of Freedom System to Disturbance $P \sin \omega t$ as a Function of ω

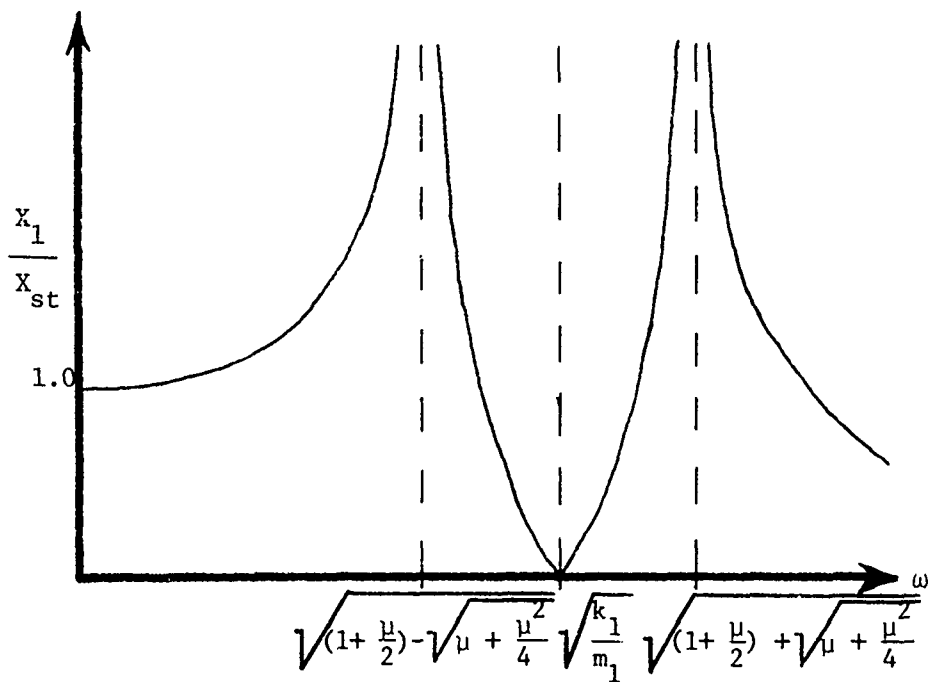


Figure 3.4

Response of Main System with Vibration Absorber Attached to Disturbance $P \sin \omega t$ as a Function of ω

The response spectrum for the main system with vibration absorber attached is shown in Figure 3.4. The system now has two natural frequencies but the vibration of the main mass at its old natural frequency is eliminated.

Den Hartog [8] shows that the new natural frequencies are dependent only on the mass ratio and are found with the following formula:

$$\left(\frac{\omega}{\omega_a}\right)^2 = \left(1 + \frac{\mu}{2}\right) \pm \sqrt{\mu + \frac{\mu^2}{4}} \quad (3.1)$$

Consider the system of Figure 3.2 in which a dashpot is arranged parallel to the vibration absorber spring k_2 , between masses m_1 and m_2 . The equations of motion for this system become

$$m_1 \ddot{x}_1 + k_1 x_1 + k_2 (x_1 - x_2) + c_2 (\dot{x}_1 - \dot{x}_2) = P \sin \omega t \quad (3.2)$$

$$m_2 \ddot{x}_2 + k_2 (x_2 - x_1) + c_2 (\dot{x}_2 - \dot{x}_1) = 0$$

Assuming the solutions

$$x_1 = X_1 e^{i\omega t} \quad (3.3)$$

$$x_2 = X_2 e^{i\omega t}$$

and substituting these into Equation (3.2) yields

$$-m_1 \omega^2 X_1 + k_1 X_1 + k_2 (X_1 - X_2) + i \omega c_2 (X_1 - X_2) = P$$

$$-m_2 \omega^2 X_2 + k_2 (X_2 - X_1) + i \omega c_2 (X_2 - X_1) = 0$$

The solution of these equations involves complex arithmetic and is lengthy. Den Hartog [8] shows the solution for the displacement of the main mass to be:

$$\frac{X_1}{X_{st}} = \sqrt{\frac{(2 \frac{c_2}{c_c} g)^2 + (g^2 - r^2)^2}{(2 \frac{c_2}{c_c} g)^2 (g^2 - 1 + \mu g^2)^2 + [\mu r^2 g^2 - (g^2 - 1)(g^2 - r^2)]^2}} \quad (3.4)$$

where

$$r = \omega a / \Omega n = \text{frequency ratio (natural frequencies)}$$

$$g = \omega / \Omega n = \text{forced frequency ratio}$$

$$c_c = 2m_2 \Omega n = \text{"critical" damping}$$

The general response spectrum for X_1/X_{st} is shown in Figure 3.5.

The shape of the response spectrum, that is the response at any input frequency, varies with the change in the parameters μ , c_2/c_c , r , and g .

The maximum value of X_1/X_{st} is

$$\frac{X_1}{X_{st}} = \sqrt{1 + \frac{2}{\mu}} \quad (3.5)$$

Note that X_1/X_{st} can be significant when μ is small.

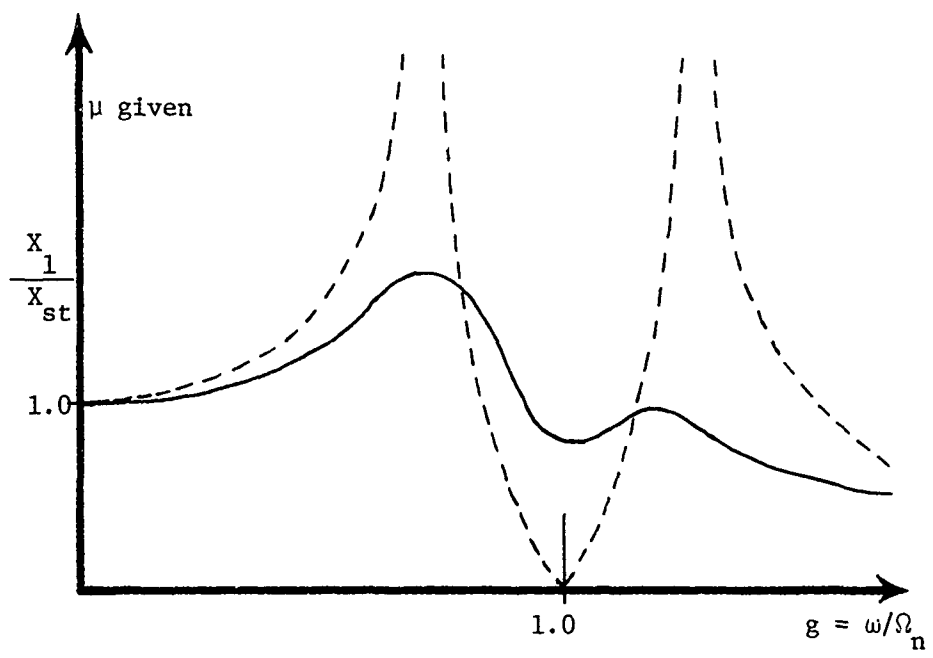


Figure 3.5

Response Curves for Motion of the Main Mass. Damped Absorber (Solid), Undamped Absorber (Dashed)

3.2 The Damped Dynamic Vibration Absorber Subject to White Noise Input

In general, mechanical systems exhibit internal damping, and often they are subject to spectral inputs rather than single sinusoids. This is the case with the offshore oil platforms under consideration. Crandall and Mark [15] carried out some parameter optimization studies with the system shown in Figure 3.6 where both the main system and the vibration absorber were damped. The system input was a white noise acceleration applied to the system foundation.

A comparison was made between the values of $E[y_1^2]/\sigma_y^2$ for various values of the system parameters where

$E[y_1^2]$ = expected value of the relative motion of m_1 with
vibration absorber attached

σ_y^2 = expected value (standard deviation) of the motion of
 m_1 without the vibration absorber

y_1 = $x_1 - x_0$

The results were similar to those obtained by Den Hartog in his work with damped vibration absorbers. Crandall found that the response depended on the mass ratio μ , the damping ratio c/c_c and the frequency ratio r .

As μ was increased the minimum value of $E[y_1^2]/\sigma_y^2$ generally decreased.

The minimum value of $E[y_1^2]/\sigma_y^2$ for each mass occurred at a frequency ratio r which followed a law such that

$$r = \frac{1}{1+\alpha\mu} \quad (3.6)$$

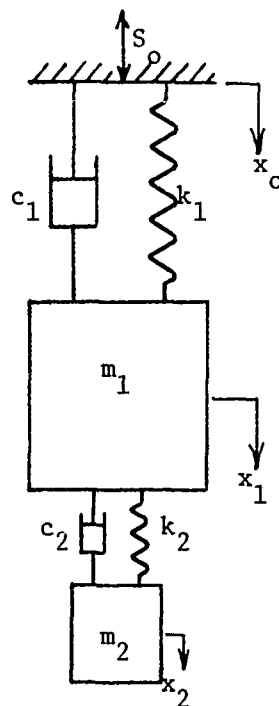


Figure 3.6

Crandall and Mark's Model Subject to
White Noise Acceleration s_0

where $\alpha > 1$ by a small amount.

The response not only depends on the damping ratio of the absorber but also the ratio of each absorber damping ratio to the main system damping ratio.

Finally, the amplitude of the absorber mass response varies inversely with the mass ratio when the system is tuned for optimum vibration absorption, and can be significant, and a limiting design factor, as the mass ratio decreases.

3.3 The Mass Damper and the Offshore Platform

The mass damper affixed to an offshore oil platform is essentially a damped vibration absorber attached to a damped vibrating system. There are two main differences between this system and those studied by Den Hartog and Crandall and Mark. First, the tower is a multi-degree of freedom system rather than a single degree of freedom system and secondly the input to the system is a varying spectral input rather than a single sinusoid or a constant white noise.

To check the feasibility of using a mass damper on an offshore tower, a modal analysis of the 1000 foot model was carried out. The details of this analysis and the complete results are in Appendix C. The results show that the model responds primarily in its fundamental mode. This indicates that the mass damper should be effective and it should be tuned to suppress the response of the first mode.

The purpose of the mass damper is to reduce the standard deviation of the response of the structure when the structure is excited by

a spectral input representing the action of the sea.

An illustrative example demonstrates the ability of the mass damper to reduce response. The model used is the 1000 foot steel jacketed tower currently being constructed by Shell Oil Corporation.

The input is the Pierson-Moskowitz wave-amplitude spectrum for a one-hundred year return sea state discretized into forty-nine frequencies as explained in Chapter 2. The one-hundred year return sea state is the sea state corresponding to a wind speed of 70 mph [16].

First the model without the mass damper was excited by the one-hundred year return sea. The results are shown for deck displacement (Figure 3.7), deck acceleration (Figure 3.8), and strain in the fourth element (Figure 3.9).

Next the mass damper was activated with the parameters in Table 3.1. The model was then excited by the same sea state. The results are shown in Figures 3.7, 3.8 and 3.9. These results are normalized to the rms response of the tower without the mass damper.

The standard deviation of each response was computed using the method outlined in Chapter 2. The standard deviations of response were reduced by the use of the damper as follows

Deck rms displacement - reduced 23.7%

Deck rms acceleration - reduced 29.2%

Top element strain - reduced 28.3%

The motion of the damper in relation to the deck was 3.42 times the motion of the deck.

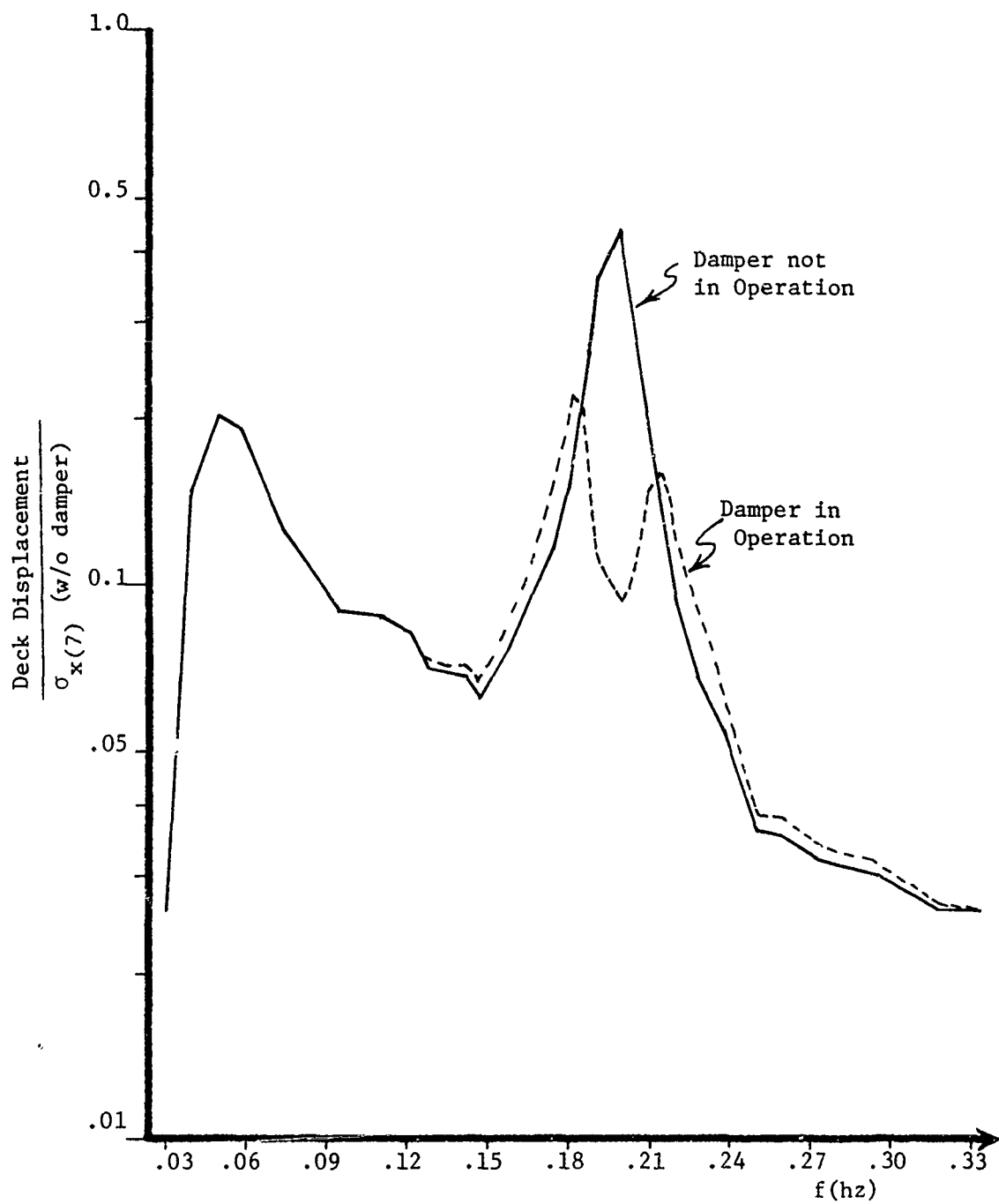


Figure 3.7

Deck Displacement vs. Frequency

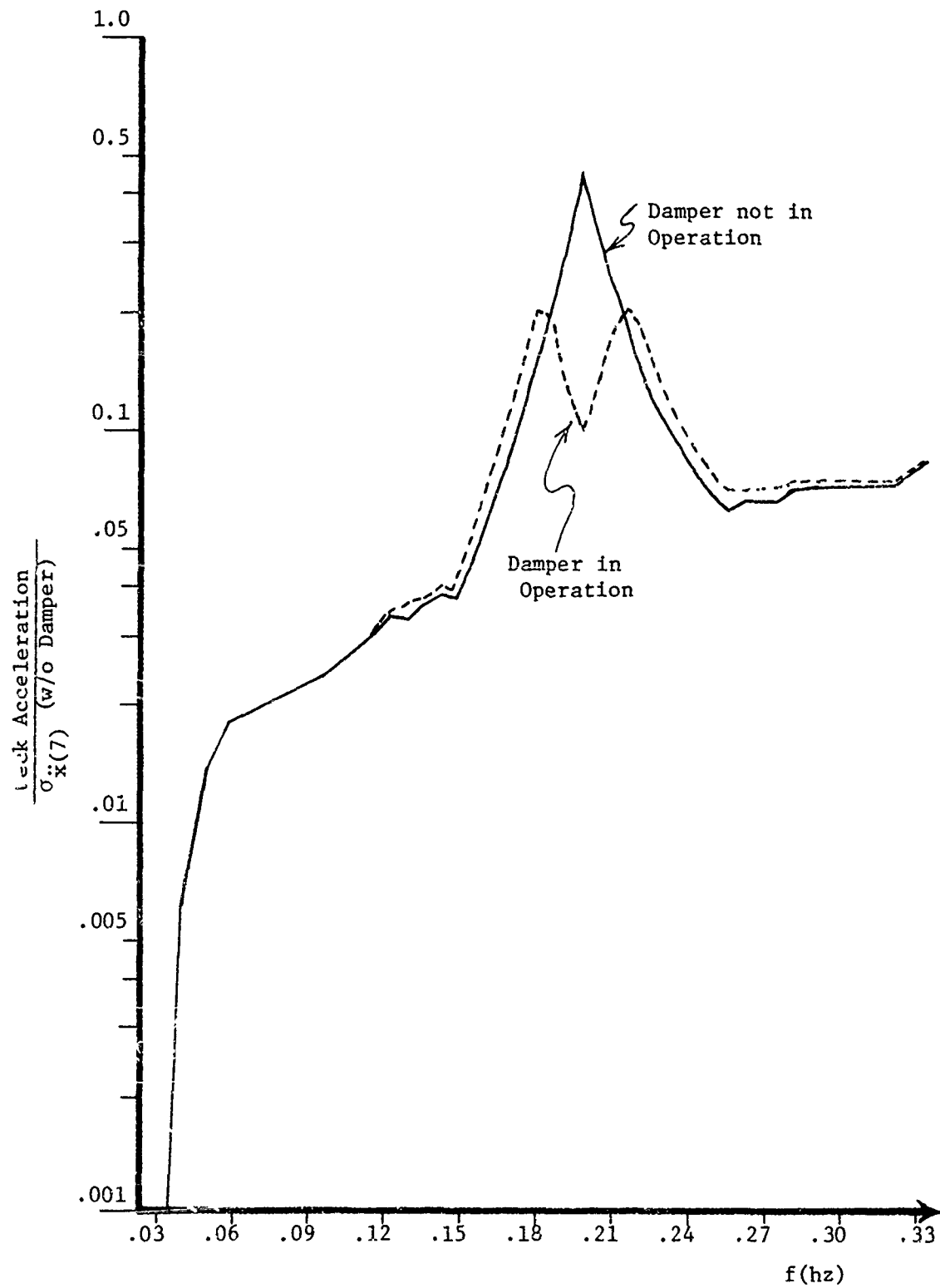


Figure 3.8

Deck Acceleration vs. Frequency

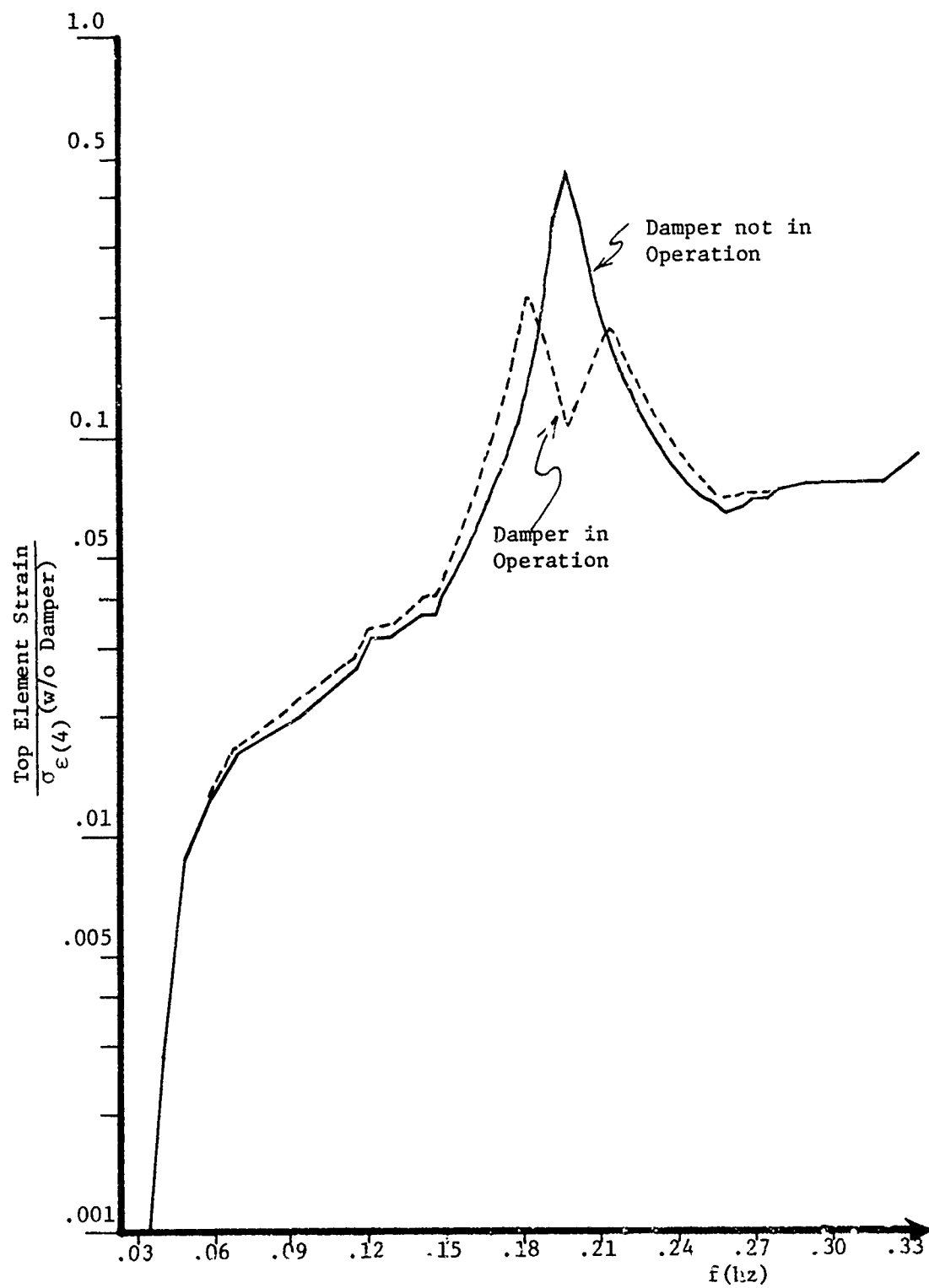


Figure 3.9
Top Element Strain vs. Frequency

μ	.01 (damper mass = $112.0 \frac{\text{MT-sec}^2}{\text{m}}$)
ω_a / Ω_n	1.00
$k_{\text{mass damper}}$	166.7 MT/m
$\frac{c_{\text{damper}}}{c_{\text{c damper}}}$	5%

Table 3.1
Mass Damper Parameters

The important variables to be examined when judging the effectiveness of the damper depend on two things. First, the space available for free travel of the damper and second, the reduction in amplitude of the response variable, for example, the element strains, which are most important for fatigue and deck acceleration, which is most important for human comfort considerations.

In this case, the damper is effective in reducing all three responses significantly, but the relative motion of the damper is probably excessive for the crowded conditions found on drilling platform decks where space is a premium.

CHAPTER 4

PARAMETER VARIATION AND SYSTEM RESPONSE

The two important factors in the design of mass dampers are the effectiveness in reducing platform response and the motion of the mass damper relative to the tower deck. The final design of a mass damper is normally a compromise between the effectiveness desired and the space allocated for movement of the damper. In this chapter the variation of these factors is studied for a range of damper parameter values. The 1000 foot tower model with eight degrees of freedom active is subjected to the 100 year return storm. Thus an extension is made from a single degree of freedom system with an attached damper studied by Den Hartog and Crandall to a mass damper in operation on a multi-degree of freedom system.

The offshore tower, while it essentially acts as a one degree of freedom system, is not, however, an idealized one degree of freedom system and it is subject to an input whose intensity varies with frequency throughout the spectrum.

There are three parameters which determine the response of the system: the mass ratio μ , the frequency ratio $\frac{\omega_a}{\Omega_n}$, and the ratio of percent critical damping in the absorber to percent critical damping in the tower β_a/β_n . The mass ratio μ , of the multi-degree of freedom system is the ratio of the damper mass to the total mass of the tower. To determine the variation in system response, each ratio is varied in turn with the other two constant. The

effectiveness of response reduction is measured as the deck displacement ratio σ_D/σ (the ratio of the rms deck displacement with mass damper to the rms deck displacement without the mass damper).

To determine the effect of mass ratio on response, $\omega a/\Omega n$ is held constant at 1.0 and βa is held at .05 (βn is constant at .03 as discussed in Chapter 2), and the mass ratio is set at .01, .03, and .05. These values of μ were chosen as being the limits and mid-point of the range of values that might be practical in this type of application. The results are shown in Figure 4.1. As μ increases, σ_D/σ decreases but the rate of decrease in σ_D/σ is decreasing. This result is similar to that predicted by MacDonald [17] in her work with Crandall's model and shows that the additional cost of an increment in μ is rewarded with a smaller increment in reduction of the deck displacement ratio. This fact is important in the economic analysis of the mass damper system.

Also plotted in Figure 4.1 is the damper displacement ratio $\frac{\sigma_{\text{damper}}}{\sigma}$ (the ratio of the rms relative mass damper displacement to the rms deck displacement without the mass damper). This ratio also decreases in the same manner as the deck displacement ratio. By increasing μ the room needed by the mass damper to operate is reduced, which again affects the cost and feasibility of the damper system.

The variation in deck displacement versus frequency for four values of μ is plotted in Figure 4.2. When $\mu \neq 0$, that is, the mass damper is in operation, the system has two resonant peaks and the response is reduced in the area of the natural frequency of the tower.

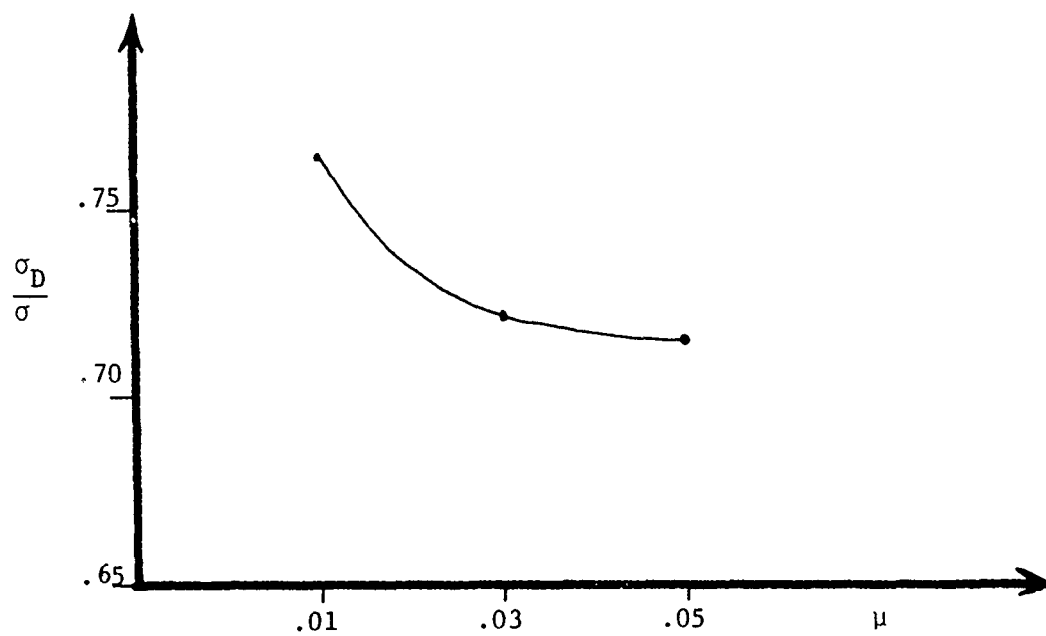
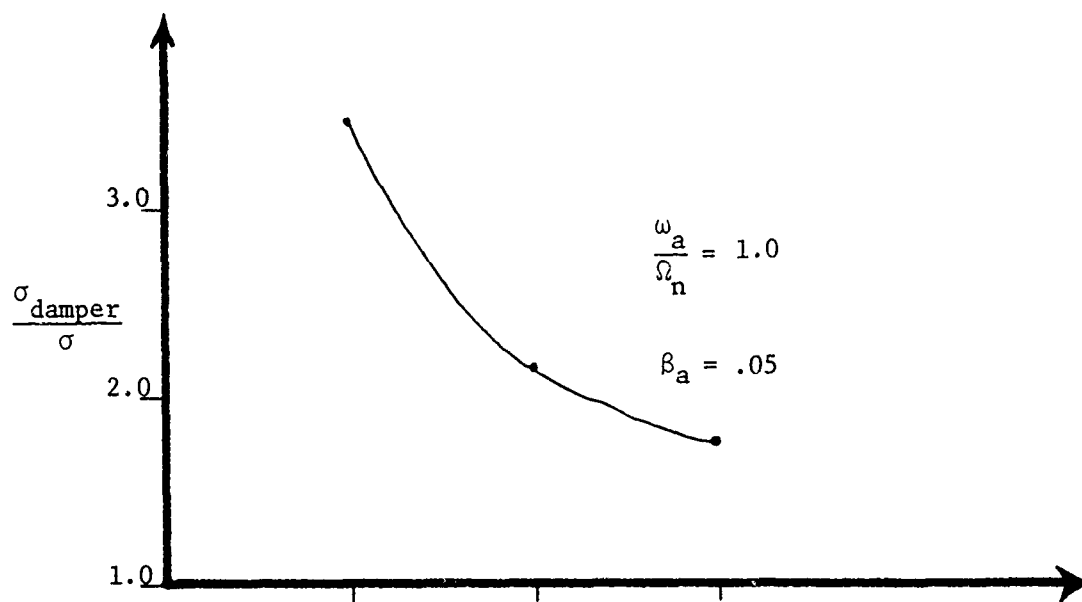


Figure 4.1

Displacement Ratios vs. Mass Ratio

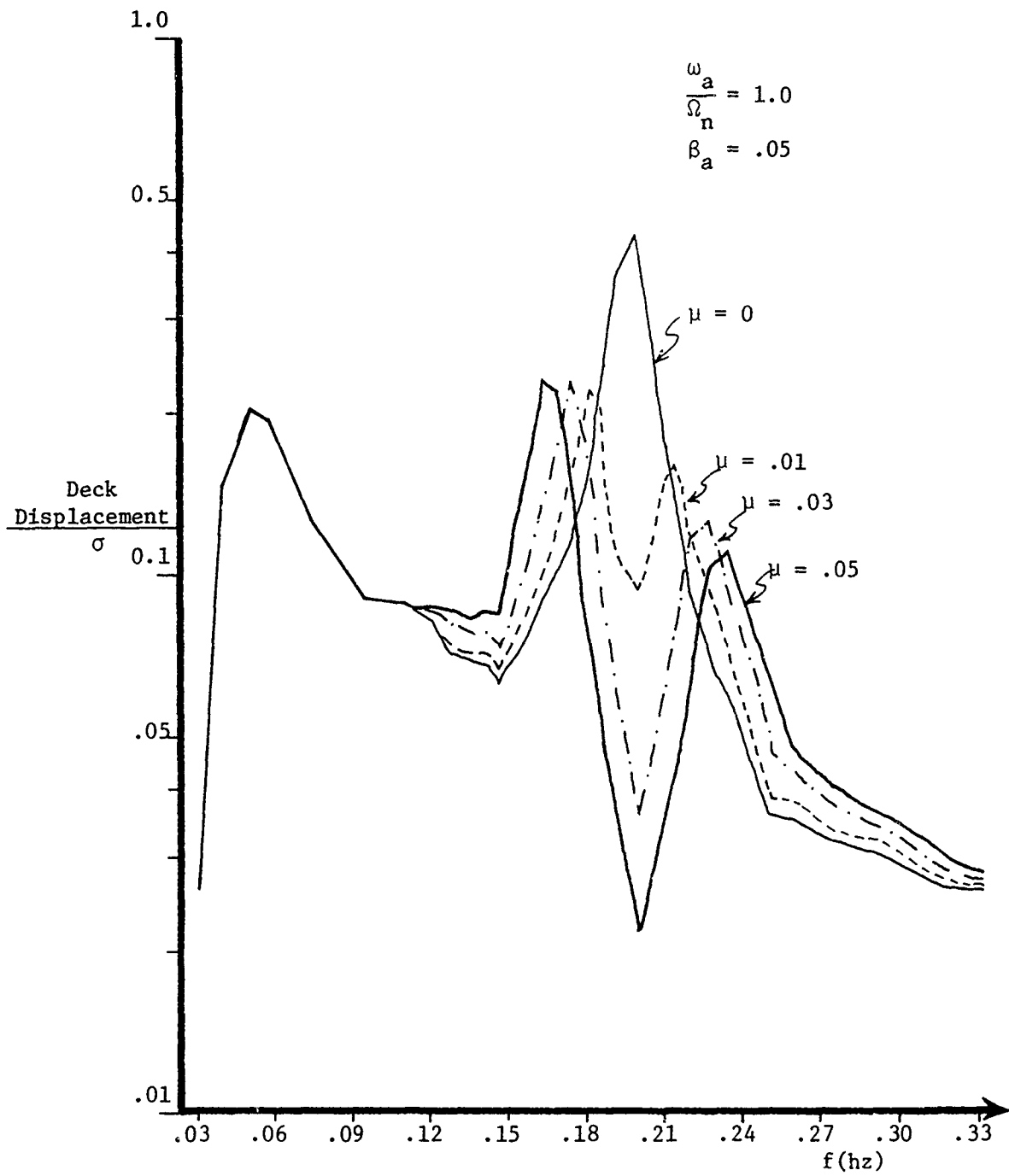


Figure 4.2
Deck Displacement vs. Frequency (μ Varying)

As μ is increased this reduction of response is increased which reduced the deck displacement ratio as shown in Figure 4.1.

To determine the impact the frequency ratio ω_a/Ω_n has on response, β_a was held constant at .05 and ω_a/Ω_n was varied for each value of μ . Figure 4.3 shows the results. The minimum values of the deck displacement ratio were achieved at the values of ω_a/Ω_n indicated by a cross on each curve.

It can be seen from Figure 4.4 where the variation in deck displacement versus frequency is plotted for values of ω_a/Ω_n , that the minimum response occurs when the two resonant peaks of the response are equal.

Returning to the results shown in Figure 4.3, note that as the mass ratio increases the deck displacement ratio becomes less sensitive to variations in the frequency ratio, allowing broader variations in tuning with little change in results.

The damper displacement ratio plotted in Figure 4.3 shows the damper displacement to be very insensitive to variations in the frequency ratio for all values of μ .

To determine the importance of the damping in the absorber on the structural response, the frequency ratio was held constant at 1.0 and the percent critical damping β_a was varied for the three values of μ . The results are plotted in Figure 4.5. Again the minimum value of the deck displacement ratios were achieved at the values of β_a indicated by a cross on each curve. Figure 4.5 shows the variation in deck displacement versus frequency for values of β_a .

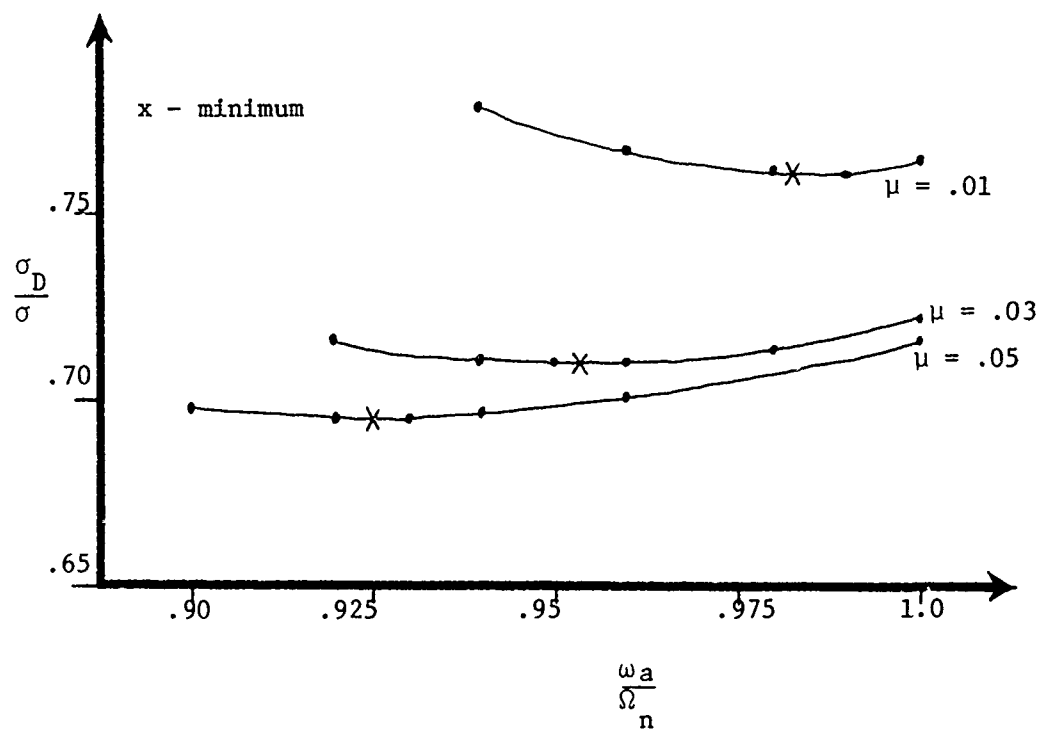
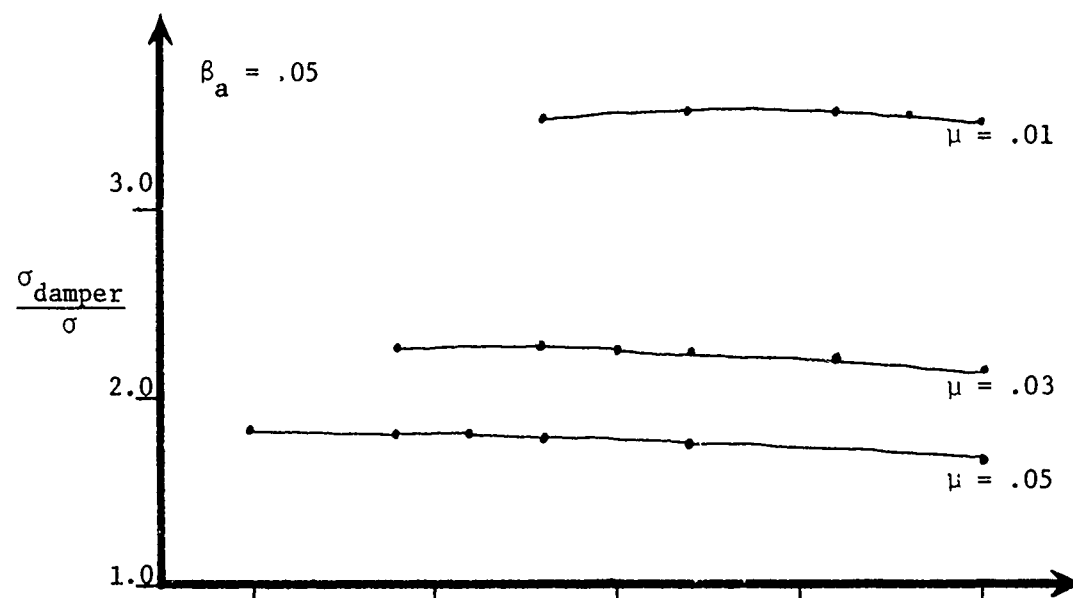


Figure 4.3

Displacement Ratios vs. Frequency Ratio

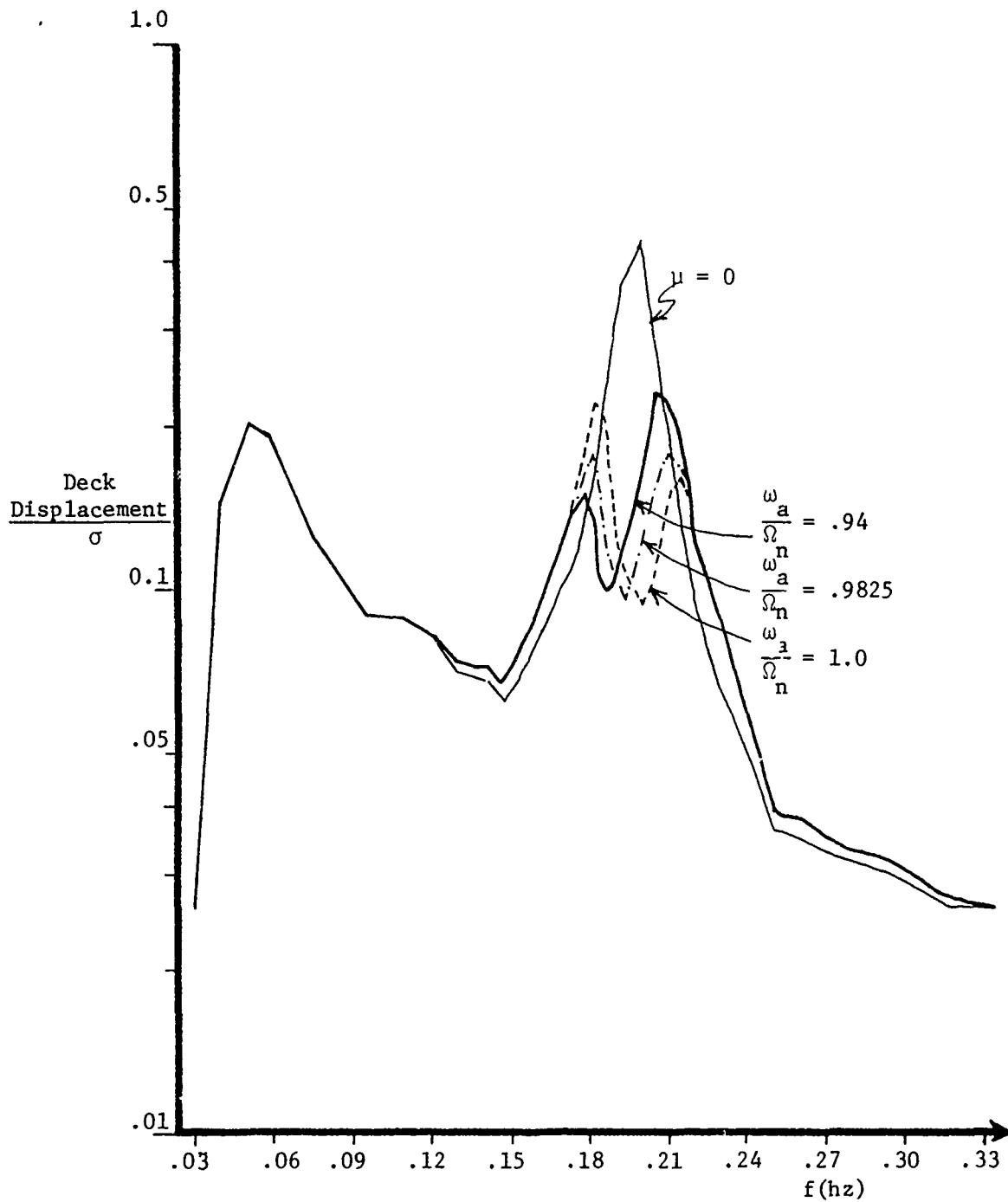


Figure 4.4

Deck Displacement vs. Frequency ($\frac{\omega_a}{\Omega_n}$ Varying)

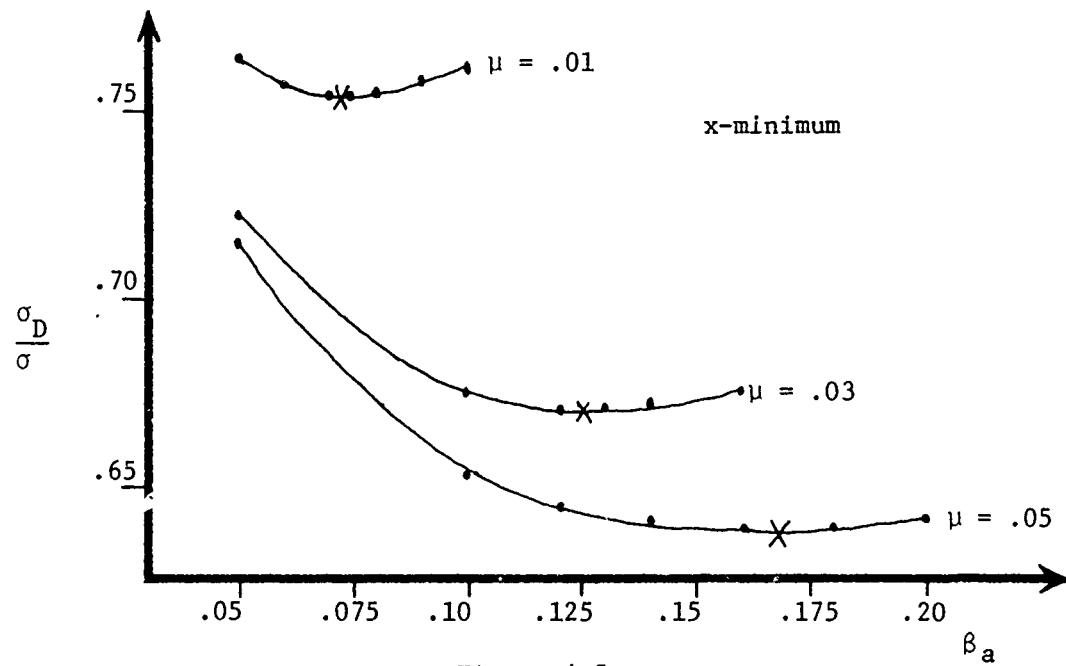
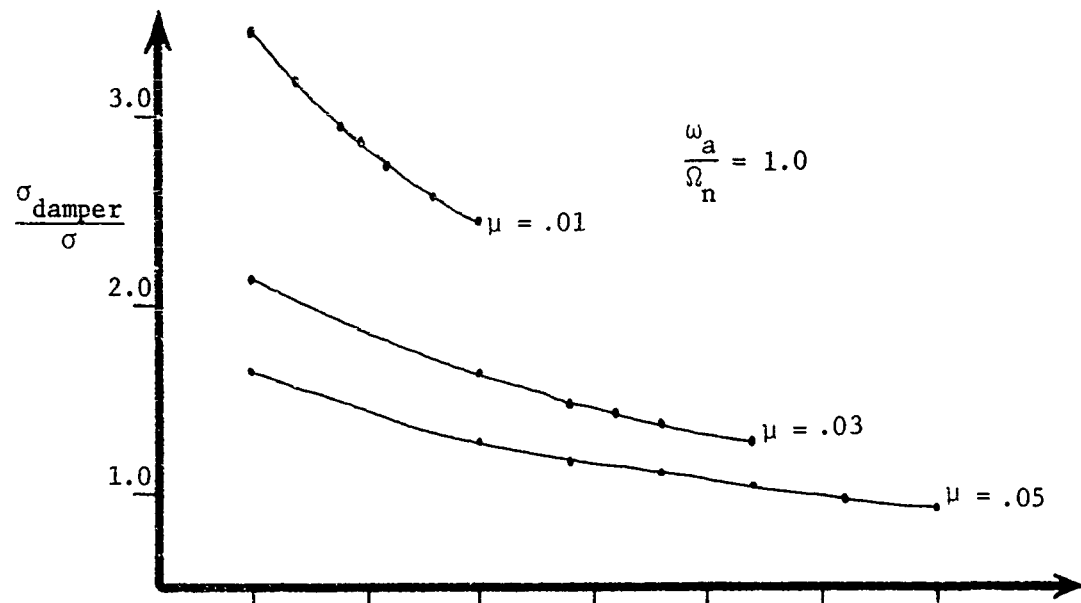


Figure 4.5
Displacement Ratios vs. β_a

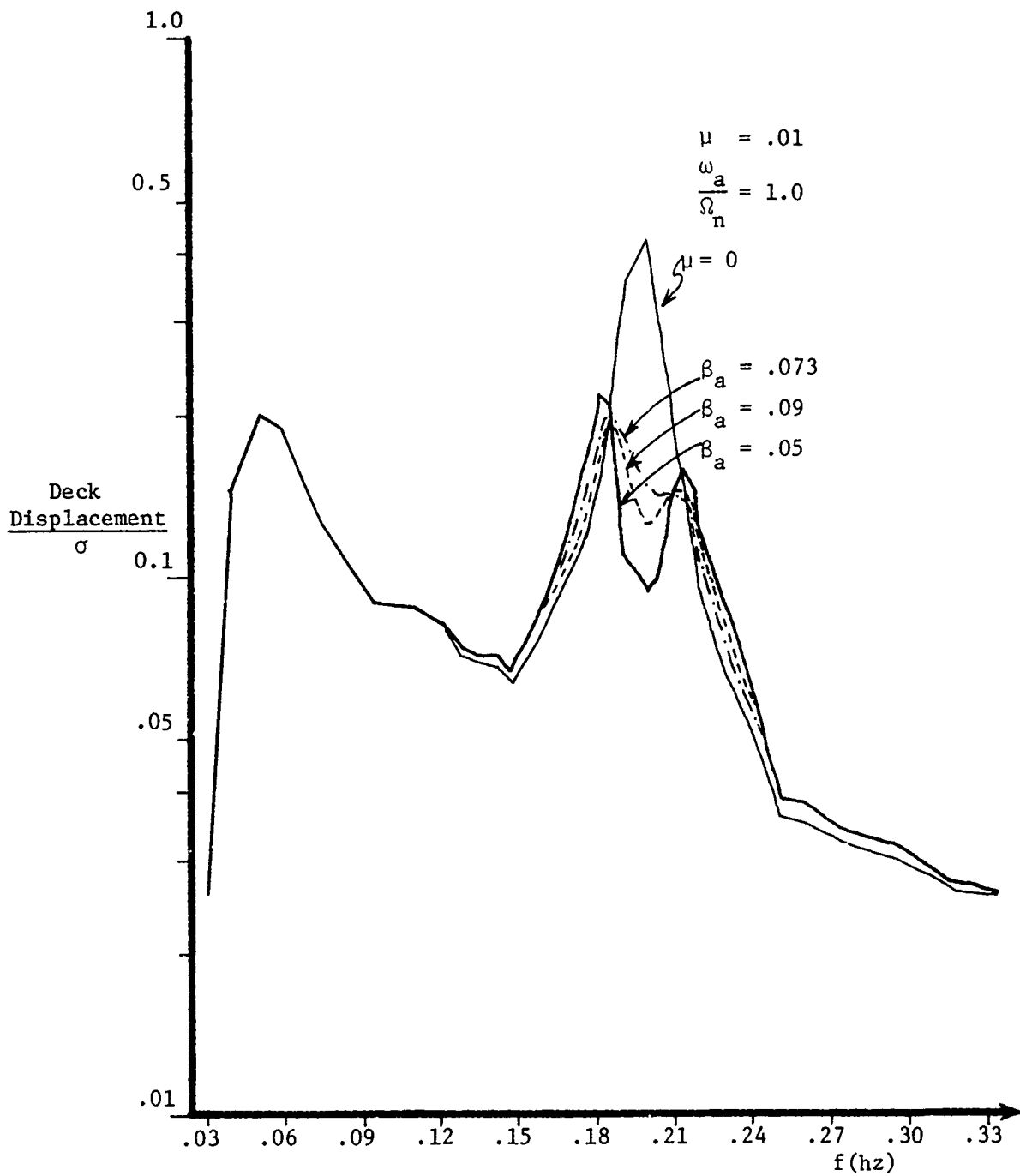


Figure 4.6
Deck Displacement vs. Frequency (β_a Varying)

The variation of damper displacement ratios is also plotted in Figure 4.5. As the value of βa increases, $\frac{\sigma_{\text{damper}}}{\sigma}$ decreases for all mass ratios. The decrease is more pronounced for $\mu = .01$. Note that although σ_D/σ varies only 1.5% in the range shown, the damper displacement ratio decreases 30%. It would seem practical, and certainly economical, to set βa at a value higher than that causing the minimum deck displacement ratio for smaller masses to reduce the damper motion without unjust penalty in deck displacement reduction.

Table 4.1 summarizes the parameter values for a mass damper utilized on offshore towers which cause a minimum in the deck displacement ratio.

μ	$\frac{\omega a}{\Omega n}$	βa
.01	.9825	.0725
.03	.9535	.1250
.05	.9260	.1675

Table 4.1
Mass Damper Parameters for Minimum Response

These results were checked to insure their validity in sea states developed from winds of 30 mph up to 100 mph. The results

remain valid without significant change because the spectra representing the various sea states are the same in the range of frequencies where resonance occurs in offshore structures.

These values cannot be considered optimum values. They do not account for the variation in relative damper displacement which must be a major factor, along with damper effectiveness, in the design of a mass damper system.

CHAPTER 5

DAMPER APPLICATION TO INDUSTRY PROBLEMS

5.1 Offshore Platforms in Water Depths Greater than 1000 Feet

As outlined in Section 1.1, offshore platforms designed for safe operation in water depths greater than 1000 feet are too expensive to be constructed in the current economic climate. This high cost results from either of two possible restrictions on the design. First, that the fundamental period of the structure be five seconds or less, or second, that if the fundamental period is allowed to be greater than five seconds, then additional reinforcing steel is required to withstand the resulting increased design loads. It appears that it might reduce the total system cost if the platform had a fundamental period greater than five seconds and the design loads were equal or less than the design loads of a platform with a fundamental period of five seconds. This second requirement permits only normal amounts of material to be used in the platform, without additional reinforcing.

To check the possible use of the tuned mass damper to help meet these two requirements, the 1200 foot steel jacketed model, with a fundamental period of 6.94 seconds, was loaded with a 100 year return sea state with and without the mass damper in operation. The damper parameters used were those listed in Table 5.1. In addition, the 1000 foot model without a mass damper was loaded with the same sea state as a basis for comparison. The responses compared

Table 5.1

Comparison of Tower Response when Subject to a
100 Year Return Sea State

Model	μ	RMS Deck Displacement*	RMS Top Element Strain**
1000 foot (T=5 sec)	0	1.000	1.000
1200 foot (T = 6.94 sec.)	0	1.158	1.012
1200 foot (T=6.94 sec.)	.01	.852	.707
1200 foot (T=6.94 sec.)	.03	.746	.596
1200 foot (T=6.94 sec.)	.05	.701	.547

* Normalized to 1000 foot model RMS deck displacement

** Normalized to 1000 foot model RMS top element strain

are RMS deck displacement and RMS top element strain. RMS deck displacement is indicative of the overall structural response and the RMS top element strain is representative of member stresses. All responses are normalized to either RMS deck displacement or RMS top element strain of the 1000 foot tower. The results are shown in Table 5.1.

The increase of tower depth to 1200 feet and fundamental period to 6.94 seconds increases the RMS deck displacement 1.158 times. The increase in RMS deck displacement is expected as the fundamental period moves to frequencies where the waves are larger. The use of the damper however reduces this response below the RMS displacement of the 1000 foot tower. The same trend is observed for RMS top element strain. When the damper is not in operation member strains in the 1200 foot model are larger than those in the 1000 foot model, thus requiring additional material to insure safety. When the damper is in operation the member strains are less than those in the 1000 foot model for all mass ratios.

Thus the two criteria are satisfied when the mass damper is applied to the 1200 foot model. The fundamental period of the structure is greater than five seconds and the member loads are less than those of a platform with a fundamental period of five seconds. Therefore the use of a tuned mass damper on a structure with a fundamental period of greater than five seconds might make the design of such a structure affordable in today's economic climate since it reduces the response.

The travel of the damper mass has not been considered in this application although it is an important design parameter. The amount of travel allowed depends on the space available, the damper mass used, and the response reduction desired. Reduced damper travel can be accomplished by increasing the damper mass or changing the damper frequency. The former, while also decreasing tower response, increases the loads on the structure caused by the additional weight. The latter increases the tower response. It is apparent in this case that there is probably a sufficient margin in response reduction at all values of μ to allow for damper motion considerations and still insure reduced costs.

5.2 Fatigue Failure in Steel Jacketed Platforms

The cyclic stresses induced in steel-jacketed deep water platforms by ocean waves in areas such as the North Sea are of sufficient magnitude on a daily basis for fatigue to be a major design consideration. As mentioned in Section 1.1, the cost of overcoming fatigue effects in such structures can be significant.

Muga and Wilson [19] present a simplified theory which can be applied to the design of ocean structures subjected to random-type forces which explains the mechanism of fatigue failure.

Assume that a fatigue curve for a structural metal has been experimentally determined under conditions similar to those of the proposed ocean structure. The results are approximately a straight

line on a plot of $\log S$ (stress) against $\log N_f$ (number of cycles of loading to failure). Figure 5.1 is a sample of such a plot. Note that the slope and intercept of the curve vary depending on material and environment.

Figure 5.1 can be used to find an estimate of the number of cycles to failure, N_{f1} , for a structural member at a given constant stress amplitude, S_1 . If the constant stress amplitude is at a constant frequency, f_1 , which would be the case in wave loading, then the time to failure, T_f , is:

$$T_f = \frac{N_1}{f_1} \quad (5.1)$$

When the stress is not of constant amplitude, but is random in nature, such as those stresses caused by ocean waves, the problem is more difficult. Empirical theory is not available, but an extrapolation of fixed amplitude fatigue data can be made as follows. Assume a specimen has been tested first at S_1 failing at N_{f1} , and then at S_2 failing at N_{f2} (see Figure 5.1). The fraction of the material's life which is used up for n_{f1} cycles at S_1 is assumed to be n_{f1}/N_{f1} . The fraction of life remaining is $1 - n_{f1}/N_{f1}$. This remaining life is assumed to be used up at stress level S_2 in n_{f2} cycles, where the fraction of life remaining is n_{f2}/N_{f2} . Thus failure occurs when

$$\frac{n_{f1}}{N_{f1}} + \frac{n_{f2}}{N_{f2}} = 1 \quad (5.2)$$

It follows that, if the specimen experiences n_{fi} cycles of

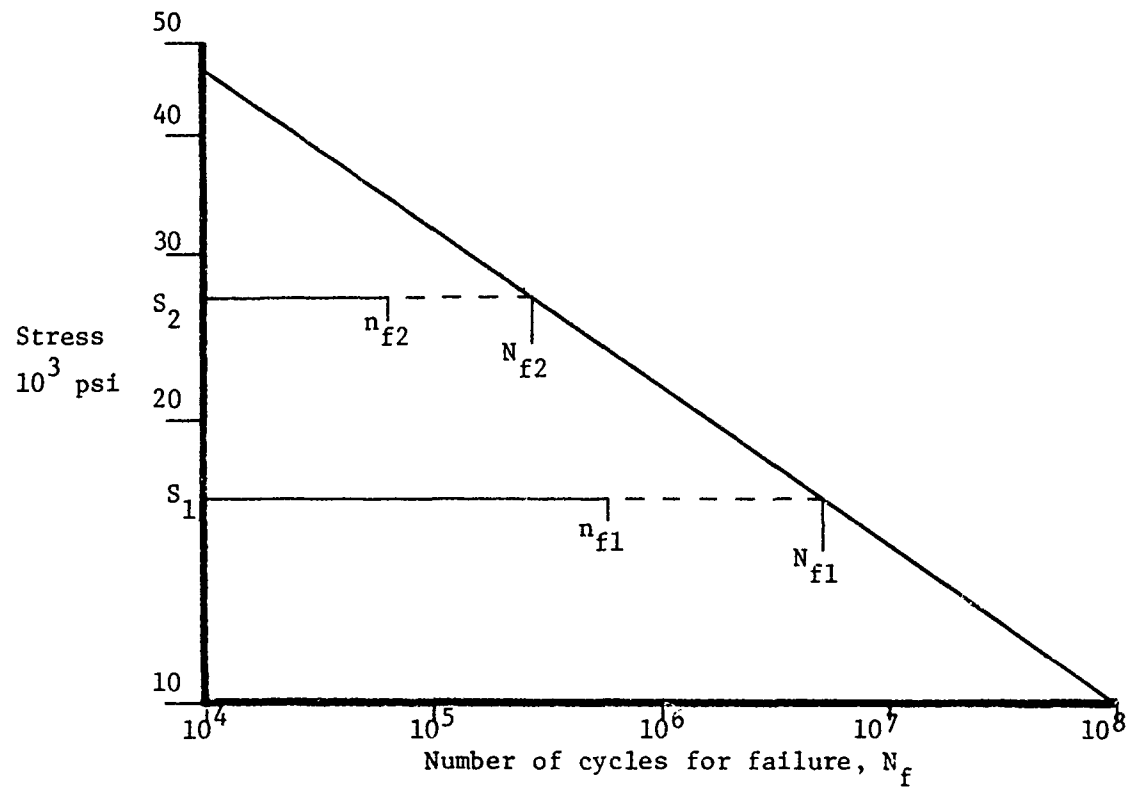


Figure 5.1

S- N_f Data in Salt Water Environment for Annealed Steel,
0.37% Carbon (21)

stress amplitude S_i for $i = 1, 2, \dots$, the total cumulative damage fraction is taken to be

$$D_f = \sum_{i=1,2,\dots} \left(\frac{n_f}{N_f}\right)_i \quad (5.3)$$

Fatigue failure occurs when $D_f = 1$.

From the above theory of fatigue failure and from Masubuchi's [19] observation that when the applied stress is lowered, the number of cycles to failure is increased, it can be concluded that when member stress levels are lowered the time to failure T_f is increased, thus increasing the life of the structure. Equation 5.1 shows this for the single stress level case. As N_{f1} increases so does T_f . For the random stress level case, Equation 5.3 shows that as the N_{fi} become larger, D_f decreases, requiring more n_{fi} before failure will occur, which in turn increases T_f .

As a corollary to the above conclusion, the time to failure can be held constant, if as stress levels are decreased, member cross sections are reduced to restore old stress levels. This allows reduction in the material used to combat fatigue affects.

The effect of a tuned mass damper on fatigue in offshore platforms was checked by loading the 1000 foot model with sea states generated by windspeeds of 30 and 40 mph (see Table 2.5). These sea states were chosen because they occur in the North Sea from 40 to 45 percent of the time [1]. RMS top element strain is the response examined as strain is a direct representation of member stresses.

The model was excited by both sea states with and without the mass damper in operation. The damper parameters used were those listed in Table 4.1. The results were normalized to the RMS strains of the structure without the mass damper and are tabulated in Table 5.2.

Note the significant reduction in RMS top element strain for all values of μ in both sea states. This reduction shows the mass damper to be very effective in reducing member stress levels which contribute to cyclic fatigue failure. Therefore it appears that the mass damper could be quite useful in increasing the fatigue life of offshore platforms or in reducing the material required in platforms to combat fatigue, thus reducing the cost of these platforms.

Again the travel of the damper mass has not been considered here, but the amount of strain reduction found allows for sufficient design margin to include allowances for damper travel.

5.3 Soil Degradation under Gravity Platforms

As outlined in Section 1.1, weakening of the soil under large gravity platforms can occur when cyclic waveloading causes pore water pressures in the soil to increase beyond a critical limit. If the loading continues, the soil becomes weaker until finally the soil liquifies and loses all bearing capacity. Several authorities [2,3,4] have done calculations in this area and they have shown that over a period of storms it is possible for the strength of the soil beneath a gravity platform such as those in operation in the

Table 5.2
 Comparison of RMS Top Element Strain for 30 and
 40 MPH Sea States

μ	RMS Top Element Strain*	
	30 MPH Sea State	40 MPH Sea State
0	1.0	1.0
.01	.703	.703
.03	.584	.586
.05	.529	.533

* Normalized to RMS Top Element Strain of Each Sea State
 without Mass Damper

North Sea to be reduced. As mentioned in Section 1.1, when this occurs the weakened foundation causes the fundamental period of the structure to increase into the range where dynamic amplification of the peak load would occur, thereby increasing the ultimate load on the structure, perhaps beyond the design load.

Analysis of soil degradation depends on three variables: the soil, the structure, and the storm loading. To determine what soil degradation could occur beneath the Condeep Brent B platform and what effect this could have on the response of the platform, preliminary analysis was carried out which used a soil model approximating that found under the Brent B platform [20], the Condeep Model described in Table 2.1, and a one-hundred year return storm described by Lee and Focht [21].

The cyclic loads on the soil were determined by loading the Condeep model with the one-hundred year return storm. These loads were then applied in a conservative manner to the soil model [22], to determine the reduction in strength of the soil after the storm. The shear modulus of the soil decreased from 5000 T/m^2 prior to the storm to 470 T/m^2 after the storm.

The shear modulus of the soil was then varied and the fundamental period of the Condeep model was determined for each value of the shear modulus. The results are plotted in Figure 5.2.

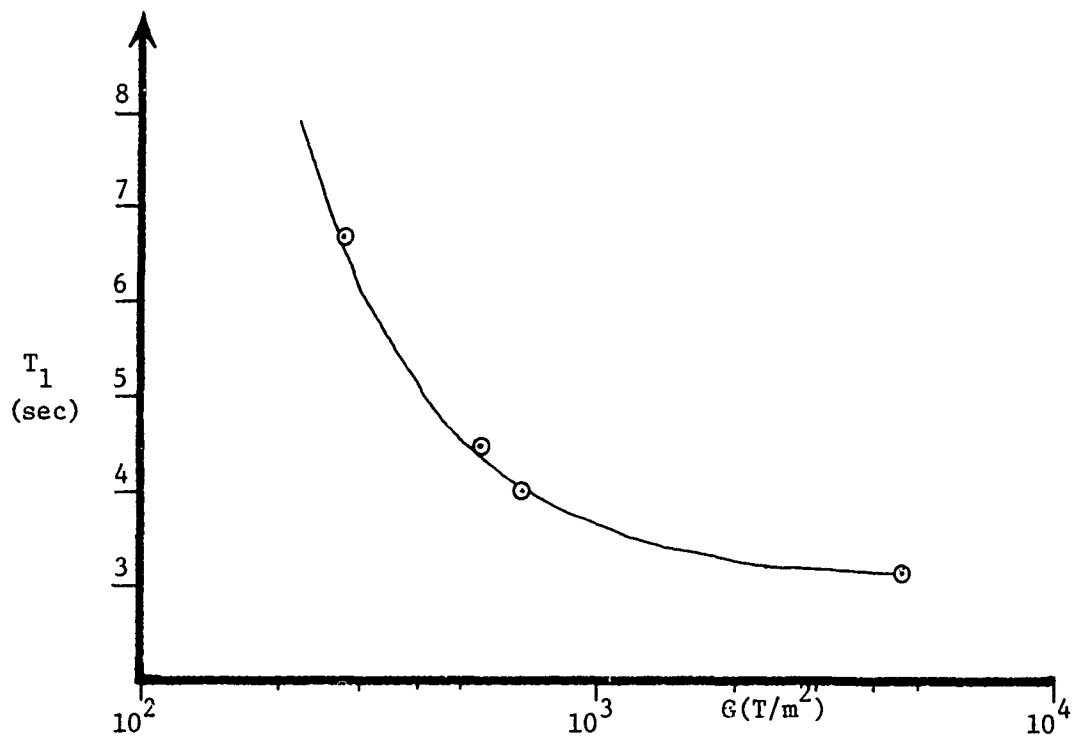


Figure 5.2
Fundamental Period vs. Shear Modulus, Condeep

To check the effectiveness of the tuned mass damper in reducing stresses caused by loads which increase as the soil degrades, the Condeep model was excited by a one hundred year return sea state after its soil had degraded to a shear modulus of 470 T/m^2 which corresponds to a fundamental period of 4.65 seconds. These results were compared to the response of the Condeep model with normal soil conditions ($G = 5000 \text{ T/m}^2$, $T_1 = 3.0 \text{ sec.}$) when excited by the same sea state. The results, normalized to the RMS responses of the Condeep under normal conditions, are listed in Table 5.3.

The RMS deck displacement has increased 1.609 times and the RMS top element strains have increased 1.239 times. Assuming the platform was designed for 100 year return conditions, the response of the platform with degraded soil is greater than allowed by design. To examine the effect of the mass damper on the response, the Condeep with degraded soil was again excited with the 100 year sea state, but with the mass damper in operation. The results for three values of μ are given in Table 5.3. Note that the damper was not able to reduce RMS displacements below design value, but the RMS strains, which are more closely related to member stresses, were reduced below design levels for all values of μ . The reduction, however, for $\mu = .01$ is only slightly below design values. If damper mass travel is considered, the long travel distances which accompany small mass ratios would probably make the use of dampers with small μ prohibitive. The results therefore show the damper to be effective only if strains are of primary importance and heavier mass ratios are used.

Table 5.3
 Comparison of Platform Response when Subject
 to 100 Year Return Sea State

Model	μ	RMS Deck Displacement*	RMS Top Element Strain**
Condeep (G=5000, T=3.0)	0	1.0	1.0
Condeep (G=470, T=4.65)	0	1.609	1.239
Condeep (G=470, T=4.65)	.01	1.292	.983
Condeep (G=470, T=4.65)	.03	1.134	.717
Condeep (G=470, T=4.65)	.05	1.055	.603

* Normalized to Condeep (G=5000, T=3.0) RMS Deck Displacement

** Normalized to Condeep (G=5000, T=3.0) RMS Top Element Strain

CHAPTER 6

SUMMARY AND CONCLUSIONS

6.1 Summary of Findings

This thesis has examined the tuned mass damper and its potential employment on an offshore platform. This examination was conducted using finite element models of three offshore platforms and discretized frequency varying spectra of three sea states.

This analysis showed that:

a) When the mass damper was applied to the platform models, the response of the platforms was reduced. The largest reductions occurred when the damper parameters were set at $\mu = .05$, $\omega_a / \Omega_n = .926$ and $\beta_a = .1675$.

b) The mass ratio μ , has the greatest effect on response reduction. As the mass ratio is increased from $\mu = .01$ to $\mu = .05$ (holding other parameters constant) the RMS deck displacement reduction changes from 23.6% to 28.6%.

c) The damper mass travel, an important design consideration, varies inversely with the mass ratio and is most affected by the damping in the mass damper.

d) The mass damper on offshore platforms in water depths greater than 1000 feet can reduce the RMS deck displacement by as much as 29.9% and the RMS strain by as much as 43.3%.

e) The mass damper can reduce the RMS strain in steel-jacketed offshore platforms subject to adverse fatigue conditions by as much as 47.1% in a 30 MPH sea and 46.7% in a 40 MPH sea.

f) When the mass damper is applied to a gravity platform subject to soil degradation the RMS strains can be reduced to levels below those for which the platform is designed.

6.2 Conclusions

The analysis in this thesis has shown the tuned mass damper on an offshore platform may be effective in reducing the high costs of platforms designed for water depths greater than 1000 feet, and fatigue in steel-jacketed platforms. It has shown the tuned mass damper to be of limited effectiveness in overcoming problems caused by soil degradation beneath gravity platforms.

While these results are based on the use of simple models, they are an initial assessment of the feasibility and effectiveness of applying a tuned mass damper to an offshore platform. The results are very encouraging. The results indicate that more detailed analyses should be undertaken, analyses which include details of specific platforms, and the economic aspects of the damper.

6.3 Areas for Further Study

An area of further study is the economics of the tuned mass damper applied to the offshore platform. A central question is - are the costs of the damper system less than the savings realized?

Another area requiring study is the effect the tuned mass damper has on reducing soil degradation and not just reducing the

effects of soil degradation.

Lastly, an area not covered in this thesis is the specific design of the mass damper for an offshore platform and the possible use and tuning of entrapped liquids in offshore platforms as damping devices.

REFERENCES

1. Kallaby, J., Price, J.B., "Evaluation of Fatigue Considerations in the Design of Framed Offshore Structures", Offshore Technology Conference, Houston, Texas, Paper OTC 2609, Volume II, 1976
2. Bjerrum, L., "Geotechnical Problems Involved in Foundations of Structures in the North Sea", Norwegian Geotechnical Institute Publication, No. 100, Oslo, 1974
3. Anderson, K., "Behavior of Clay Subject to Undrained Cyclic Loading", Behavior of Offshore Structures '76, Trondheim, Norway, Volume I, 1976
4. Hoeg, K., "Foundation Engineering for Fixed Offshore Structures", Behavior of Offshore Structures '76, Trondheim, Norway, Volume I, 1976
5. Taylor, R.E., "A Preliminary Study of the Structural Dynamics of Gravity Platforms", Offshore Technology Conference, Houston, Texas, Paper OTC 2406, Volume III, 1975
6. Watt, B.J., et al, "Response of Concrete Gravity Platforms to Earthquake Excitations", Offshore Technology Conference, Houston, Texas, Paper OTC 2673, Volume III, 1976
7. Utt, M.E., et al, "Estimation of the Foundation Condition of a Fixed Platform by Measurement of Dynamic Response", Offshore Technology Conference, Houston, Texas, Paper OTC 2625, Volume III, 1976
8. DenHartog, J.P., Mechanical Vibrations, McGraw Hill, New York, 1956
9. DuVall, W., "Approximate Models for Offshore Concrete Gravity Structures", M.S. Thesis, M.I.T., 1976
10. Nath, J.H., "The Dynamic Response of Fixed Offshore Structures to Periodic and Random Waves", Ph.D. Thesis, M.I.T., 1967
11. Maddox, "Fatigue Analysis for Deepwater Platforms", Offshore Technology Conference, Houston, Texas, Paper OTC 2051, Volume II, 1974

12. Zijp, D., et al, "Dynamic Analysis of Gravity Type Offshore Platforms Experience, Development and Practical Application", Offshore Technology Conference, Houston, Texas, Paper OTC 2433, Volume I, 1976
13. Kinsman, B., Windwaves, Prentice-Hall, New York, 1965
14. Pierson, W., McSkowitz, L., "A Proposed Spectral Form for Fully Developed Wind Seas Based on the Similarity Theory of S.K. Kitaigorodskii", Journal of Geophysical Research, Volume 69, No. 24, December 15, 1964
15. Crandall, S., Mark, W., Random Vibration in Mechanical Systems, Academic Press, New York, 1963
16. Whitehead, H., An A-Z of Offshore Oil and Gas, Kogan Page, Ltd., London, 1976
17. MacDonald, R.L., "Application of a Tuned Mass Damper in Reducing the Wind-Induced Motion of a Tall Building", M.S. Thesis, M.I.T., 1976
18. Muga, B.J., Wilson, J.F., Dynamic Analysis of Ocean Structures, Plenum Press, New York, 1970
19. Masubuchi, K., Materials for Ocean Engineering, M.I.T. Press, Cambridge, 1970
20. Eide, O.T., Larsen, L.G., "Installation of the Shell/Esso Brent B Condeep Production Platform", Offshore Technology Conference, Houston, Texas, Paper OTC 2434, Volume I, 1976
21. Lee, K.L., Focht, J.A., "Liquification Potential at Ekofisk", Journal of the Geotechnical Division, ASCE, GT1, January, 1975
22. Anderson, K.H., "Research Project, Repeated Loading on Clay", Norwegian Geotechnical Institute Publication, No. 74037-9, Oslo, 1975
23. Biggs, J.M., Introduction to Structural Dynamics, McGraw Hill, New York, 1964
24. Malhotra, A.K., Penzien, J., "Response of Offshore Structures to Random Wave Forces", Journal of the Structural Division, ASCE, ST 10, October 1970
25. Millman, D.N., "A Dynamic Analysis of A Fixed Offshore Drilling Structure Subject to Random Waves", M.S. Thesis, M.I.T., 1973

APPENDIX A
COMPUTER PROGRAM LISTING

```

C      * MAIN PROGRAM *
C      COMPLEX A,B
C      REAL MASS, LENGHT
C      DIMENSION TOWER (20), FREQ (100), MASS (200), STIFF(2
*00), A (200), B(50), DIS (50), VEL (50), ACC (50), R (50),
*S(50),H(50),PHASE(50),Q(500),P(50)
C      DATA IR, IW /8,5/
C      INPUT DATA
C      CALL INPUT (IR, IW, TOWER, NELEM, NFREQ,
*HEIGHT,ZO,REB,RET,RIB,RIT,DEPTH,E,RO,DMASS,DINER,FREQ,
*H,PHASE,DI,TIME,NRIGD,KQ,KD,KM,ALPHA,BETAV,BETAH,DK,DM,BETAD,KNW)
C      STIFFNESS AND MASS MATRICES
C      CALL ASMBL (NELEM, NEQ, MBW,
*HEIGHT, REB, RET, RIB, RII, E, RO, DMASS, DINER, STIFF, MASS, KQ,
*NRIGD, IR, IW, DEPTH, KD, DM, DK, KM, LENGHT, DA, DB)
C      TIME OR FREQUENCY DOMAIN ANALYSIS
C      IF ( NFREQ.GE.0 ) GO TO 12
C      NFREQ = - NFREQ
C      FREQUENCY DOMAIN ANALYSIS
C      CALL TF (IW, TOWER, NELEM, HEIGHT, ZO, RET, REB, DEPTH,
*NEQ, MBW, STIFF, MASS, A, B, FREQ, KQ, NRIGD, H, BETAV, BETAH, ALPHA,
*KD, LENGHT, DA, DB, RIT, S, BETAD, DK, DM, NFREQ, KNW)
C      STOP
C      DYNAMIC ANALYSIS IN TIME DOMAIN
C      12 IF ( NFREQ .EQ. 0 ) STOP
C      CALL TIME H ( IW, NEQ, MBW, NFREQ, NELEM,
*RET, REB, HEIGHT, ZO, DEPTH, DI, TIME,
*STIFF, MASS, FREQ, A, B, H, PHASE,
*DIS, VEL, ACC, R, S, P, Q, KQ, NRIGD )
C      STOP
C      END

```

```

MP 00
MP 01
MP 01A *
MP 03
MP 05
MP 06
MP 06A
MP 07
MP 08
MP 09
MP 12
MP 12A *
MP 14
MP 15A
MP 16
MP 16A
MP 16B
MP 16C
MP 16D
MP 17
MP 18

```

```

C SUBROUTINE INPUT
SUBROUTINE INPUT (IR, IH, TOWER, NELEM, NFREQ,
*HEIGHT, Z0, REB, RET, RIB, RIT, DEPTH, E, RC, DMASS, DINER, FREQ,
*R, PHASE, DT, TIME, NRIGD, KQ, KD, KM, ALPHA, BETAV, BETAH, DK, DM, BETAD, KNW)
DIMENSION TOWER(20), FREQ(1), H(1), PHASE(1)
C
C READ TOWER AND CONTROL CARD
READ (IR,1) TOWER, NELEM, NFREQ, NRIGD, KQ, KD, KM, KNW
WRITE (IW,2) TOWER, NELEM, NFREQ
IF (K2.NE.0) WRITE (IW,50)
50 FORMAT (//5X, ' EARTHQUAKE OPTION IS IN EFFECT')
IF (KD.NE.0) WRITE (IW,51)
51 FORMAT (//5X, ' DAMPER OPTION IS IN EFFECT')
C
C READ OVERALL DIMENSIONS
READ (IR,3) HEIGHT, Z0, REB, RET, RIB, RIT, DEPTH
WRITE (IW,4) HEIGHT, Z0, REB, RET, RIB, RIT, DEPTH
C
C READ MATERIAL PROPERTIES
READ (IR,3) E, RO
WRITE (IW,5) E, RC
C
C READ ALPHA, BETAV, BETAH FOR DAMPING. IF NO DAMPING READ IN ZERO V
READ (IR,3) ALPHA, BETAV, BETAH
WRITE (IW,21) ALPHA, BETAV, BETAH
C
C READ DECK LOAD
READ (IR,3) DMASS, DINER
WRITE (IW,6) DMASS, DINER
C
IF (KD.EQ.0) GO TO 22
READ (IR,41) DM, OMEGA, BETAD
DK=OMEGA**2*DM

```

```

SI 00
SI 01
SI 02
SI 03
SI 05
SI 06
SI 08
SI 09
SI 10
SI 11
SI 12
SI 13
SI 14
SI 15
SI 16
ALUE
SI 17
SI 18
SI 19
SI 20

```

```

*
*
*
*
*
*
*
*
*

```

```

WRITE(IH,42) DK,DM,OMEGA,BETAD
41 FORMAT (3F8.4)
42 FORMAT(4X, 'DAMPING PARAMETERS',/2X, 'SPRING CONSTANT =',F10.4/2X,
* 'DAMPER MASS =',F8.4/2X, 'DAMPER FREQUENCY (RAD/SEC) =',F8.4/
*2X, ' PERCENT CRITICAL DAMPING =',F8.4)
22 CONTINUE
C READ FREQUENCIES
IF ( NFREQ .GE. 0 ) GO TO 10
C READ FREQUENCIES FOR STATIC RESPONSE IN FREQUENCY DOMAIN
N = -NFREQ
READ (IR,3) (FREQ(I),H(I), I= 1,N )
WRITE (IW,7) (FREQ(I),H(I), I= 1,N )
RETURN
C READ TIME AND TIME INTERVAL PLUS CONDENSED SPECTRUM PARAMETERS
C FOR DYNAMIC ANALYSIS
10 IF ( NFREQ .LE. 0 ) GO TO 12
READ ( IR , 3 ) DT , TIME
WRITE ( IW , 8 ) DT , TIME
DO 1; I = 1,NFREQ
11 READ ( IR , 3 ) FREQ(I) , H(I) , PHASE(I)
WRITE ( IW , 9 ) (FREQ(I) , H(I) , PHASE(I) , I = 1,NFREQ )
12 RETURN
C
1 FORMAT (20A4,/, 7I4)
2 FORMAT (.1,/,5X, 20A4,/,/,
* 5X, I5, ' ELEMENTS' , / , 5X, I5, ' FREQUENCIES' , /)
3 FORMAT (10F8.2)
4 FORMAT (//5X, '*OVERALL DIMENSIONS*',//
*5X, 'TOWER HEIGHT' , , F8.2, ' M.'//
*5X, 'CAISSON HEIGHT' , , F8.2, ' M.'//
*5X, 'EXTERNAL RADIUS AT THE BOTTOM' , , F7.2, ' M.'//
*5X, 'EXTERNAL RADIUS AT THE TOP' , , F7.2, ' M.'//
*5X, 'INTERNAL RADIUS AT THE BOTTOM' , , F7.2, ' M.'//

```

```

SI 21
SI 22
SI 23
SI 24
*
SI 27
SI 28
SI 28A
SI 29
SI 29A
SI 29B
SI 30
SI 30A
SI 30B
SI 31
SI 32
*
SI 34
SI 35
*
SI 37
SI 38
SI 39
SI 40
SI 41
SI 42

```

```

*5X, 'INTERNAL RADIUS AT THE TOP', F7.2, 'M.'//
*5X, 'DEPTH OF WATER', F8.2, 'M.'//
5 FORMAT (///5X, '**MATERIAL PROPERTIES**//
*5X, 'E =', E10.3/5X, 'RO =', E10.3/)
6 FORMAT (///5X, 'DECK MASS', E12.4/
5X, 'DECK INERTIA', E12.4/)
7 FORMAT (///5X, '**CONDENSED SPECTRUM PARAMETERS * '///3X, ' FREQ', 8X
** WAVE HEIGHT'//(3X, 2F15.4))
8 FORMAT (///5X, '* TIME INTERVAL AND TOTAL TIME * '///5X,
* DELTA T =', F7.3/5X, 'TIME =', F7.3/ )
9 FORMAT ( ///5X, '* CONDENSED SPECTRUM PARAMETERS * '///13X,
* FREQ', 8X, 'WAVE HEIGHT', 3X, 'PHASE ANGLE'//(3X, 3F15.4))
21 FORMAT (///5X, '* DAMPING COEFFICIENTS * '///5X, ' ALPHA =', E10.3/5X
* BETA =', E10.3/5X, ' BETAH =', E10.3/)

```

88 C
END

```

SI 43
SI 44
SI 45
SI 46
SI 47
SI 48
,
SI 50
SI 51
SI 52
SI 52A
,
SI 53
SI 54

```



```

C          SUBROUTINE ASMBL (NELEM, NEQ, MBW,
C          SUBROUTINE ASHBL (NELEM, NEQ, MBW,
C          *HEIGHT, REB, RET, RIB, RIT, E, RO, DMASS, DNER, STIFF, MASS, K2,
C          *NRIGD, IR, IW, DEPTH, KD, DM, DK, KM, LENGHT, DA, DB)
C          REAL MASS, LENGHT, MG
C          DIMENSION STIFF(200), MASS(200), A(10), AMAS(12,12), STIF(12,12)
C
C          INITIALIZE
C          NEO = 2*(NELEM + 1)
C          IF(KO.NE.0) NEQ=NEQ+2
C          IF (KD .NE. 0) NEQ=NEQ+1
C          MBW = 4
C          LIM = NEQ * MBW
C          DO 10 I = 1, LIM
C             STIFF(I) = 0.
C             10 MASS (I) = 0.
C
C          COMPUTE ELEMENT MATRICES AND ASSEMBLE
C          DR = NELEM
C          LENGHT = HEIGHT/DN
C          DA = (RET-REB)/DN
C          DB = (RIT-RIB) / DN
C          A1 = REB
C          B1 = RIB
C          EMASS = DMASS
C          IF (KD .NE. 0) EMASS= EMASS + DM
C
C          DO 12 N = 1, NELEM
C             A2 = A1 + DA
C             B2 = B1 + DB
C             CALL SUBK (E,A1,B1,A2,B2,LENGHT, A )
C             CALL ADD (NEQ ,STIFF , N , A )
C             CALL SUBM (RO,A1,B1,A2,B2,LENGHT, EMASS, A )

```

```

SAS 00
SAS 01
*
*
*
SAS 06
SAS 07
SAS 08
SAS 09
SAS 10
SAS 11
SAS 12
SAS 13
SAS 14
SAS 15
SAS 16
SAS 17
SAS 18
SAS 19
SAS 20
SAS 21
SAS 22
*
SAS 23
SAS 24
SAS 25
SAS 26
SAS 27
SAS 28
SAS 29

```

SAS 30
 SAS 31
 SAS 32
 SAS 33
 SAS 34
 SAS 35
 SAS 36
 SAS 37
 SAS 38
 SAS 39
 SAS 40
 SAS 41
 SAS 42
 SAS 43
 SAS 44
 SAS 45
 SAS 46
 SAS 47

```

CALL ADD (NEQ ,MASS, N, A )
A1 = A2
12 B1 = B2
C
C ADD DECK MASS
I = 2 * NELEM
MASS (I+1) = MASS(I+1) + DMASS
MASS (I+2) = MASS (I+2) + DINER
C
A1 = REB
B1 = RIB
DO 14 M = 1, NELEM
A2 = A1 + DA
B2 = B1 + DB
CALL SUBKG (RO, REB, RIB, A1, B1, A2, B2, LENGHT, EMASS, M,A )
CALL ADD (NEQ, STIFF, M, A)
A1 = A2
14 B1 = B2
IF(NRIGD.NE.0) GO TO 35
READ (IR,36) GS,ROS,HH,CC,DC,PNU,BL,PR,ROC
WRITE (IW,37) 3S,PNU,ROS,HH,CC,DC,BL,BR,ROC
36 FORMAT(9F8.4)
37 FORMAT(4X,'SOIL PROPERTIES'/2X,'SHEAR MODULAS =',F8.2/2X,'POI
1SSONS RATIO =',F8.2/2X,'DENSITY =',F8.2//4X,'DIMENSIONS OF
2 CAISSON'/2X,'HEIGHT =',F8.2/2X,'WIDTH =',F8.2/2X,'LENG
3TH =',F8.2//2X,'MASS RATIO, HORIZONTAL =',F8.2/2X,'MASS RATIO
4, ROCKING =',F8.2/2X,'MASS RATIOS FOUND FROM GRAPH,P.351,RICHAR
5T'/2X,'DENSITY OF CAISSON =',F8.2)
*** CALCULATE KL AND K0 *****
SKL=2.0*(1.0+PNU)*GS*BL*(CC*DC)**0.5
SKO=(GS/1.0-PNU)*BR*CC*(DC**2)
*** MASS AND INERTIA OF CAISSON *****
CHASS=ROC*CC*DC*HH

```

```

CINER=((DC*(HH/2.0)**3)/12.0)*ROC*CC
FT=EMASS*9.81
WRITE (IW,42) FT
42 FORMAT (2X,'LOAD ON CAISSON =',E10.2/)
C *** EARTHQUAKE OPTION *****
IQ=0
IF(KQ.NE.0) IQ=2
I=1+IQ
J=2+IQ
K=NEQ+1+IQ
C *** MODIFY MATRICES *****
STIFF(I)=STIFF(I)+SKL
STIFF(J)=STIFF(J)+SKL*HH*HH+SKO-FT*HH
STIFF(K)=STIFF(K)+SKL*HH
MASS(I)=HASS(I)+CMASS
MASS(J)=MASS(J)+HH*HH*CMASS/2.0+2.0*(CINER+(HH/2.0)*DC*(HH/4.0)**2
*)
MASS(K)=MASS(K)+HH*CMASS/2.0
WRITE (IW,39) GS,SKL,SKO,CMASS
39 FORMAT (2X,'SHEAR MODULUS =',E10.2/2X,'EFFECTIVE SPRING CONSTANTS
1'/2X,'HORIZONTAL ',4X,E10.2/2X,'ROTATIONAL ',4X,E10.2/2X,'MASS
2 OF CAISSON ',4X,E10.2)
35 IF (KD.EQ. 0) GO TO 40
C MODIFY MATRICES FOR MASS DAMPER
I=NEQ-2
J=NEQ
K=3*NEQ-2
STIFF(I)=STIFF(I)+DK
STIFF(J)=DK
STIFF(K)=-DK
MASS(J)=DM
40 CONTINUE
IF(KQ.EQ.0) GO TO 41

```

```

C
STIFF(1)=SKL
STIFF(2)=SKO
*** MODIFICATIONS FOR MASS MATRIX *****
REQM=((DC*CC)/3.14159)**0.5
REQI=(DC*CC**3)/(3.0*3.14159)**0.25
MG=(0.77*ROS*(REQM**3))/(2.0-PNU)
YG=(1.92*ROS*(REQI**5))/(3.0*(1.0-PNU))
MASS(1)=MG
MASS(2)=YG
41 IF(KM.EQ.0) GO TO 43
C
PRINT OUT MASS AND STIFFNESS MATRICES
WRITE(IW,29)
29 FORMAT('//10X, ' MASS MATRIX'//)
DO 100 I=1,NEQ
DO 75 J=1,NEQ
75 AMAS(I,J)=0.
100 CONTINUE
DO 101 I=1,NEQ
K=I+3
DO 76 J=I,K
IJ=(J-I)*NEQ+I
76 AMAS(I,J)=MASS(IJ)
101 CONTINUE
DO 102 I=1,NEQ
K=I+1
L=I+3
DO 77 J=K,L
77 AMAS(J,I)=AMAS(I,J)
102 CONTINUE
DO 30 I=1,NEQ
WRITE (IW,31)(AMAS(I,J),J=1,NFQ)
31 FORMAT(/11(1X,E10.2))
30 CONTINUE

```

```

WRITE (IW,32) , STIFFNESS MATRIX'//)
32 FORMAT(//10X,
DO 103 I=1,NEQ
DO 78 J=1,NEQ
78 STIF(I,J)=0.
103 CONTINUE
DO 104 I=1,NEQ
K=I+3
DO 79 J=I,K
IJ=(J-I)*NEQ+I
79 STIF(I,J)=STIFF(IJ)
104 CONTINUE
DO 105 I=1,NEQ
K=I+1
L=I+3
DO 80 J=K,L
80 STIF(J,I)=STIF(I,J)
105 CONTINUE
DO 28 I=1,NEQ
WRITE (IW,27)(STIF(I,J),J=1,NEQ)
27 FORMAT(/11E10.3)
28 CONTINUE
43 RETURN
END

```

SAS 49

```

C
SUBROUTINE SUBK (E,A1,B1,A2,B2,LENGHT,STIFF)
SUBROUTINE SUBK (E,A1,B1,A2,B2,LENGHT,STIFF)
REAL LENGHT
DIMENSION A(5), W(5), F(4), STIFF(10)
DATA A,W / 0., -538469, .538469, -.906180, .906180, .553889,
*2*.478629, 2*.236927 /
DO 1 I = 1,10
1 STIFF(I) = 0.
DO 2 N = 1,5
X = A(N)
X = .5*(X+1.)
F(1) = 12.*X-6.
F(3) = -F(1)
F(2) = (-4.+ 6.*X)*LENGHT
F(4) = (-2.+6.*X)*LENGHT
AA = A1*(1.-X)+A2*X
B = B1*(1.-X)+B2*X
C = 0.7853981 * (A**4-B**4)/LENGHT**3/2.*W(N)*E
IJ = J
DO 2 J = 1,4
DO 2 I = 1,J
IJ = IJ+1
2 STIFF(IJ) = STIFF(IJ) + C*F(I)*F(J)
RETURN
END

```

```

SK 00
SK 01
SK 03
SK 04
SK 04A
SK 05
SK 06
SK 07
SK 08
SK 09
SK 10
SK 11
SK 12
SK 13
SK 14
SK 15
SK 16
SK 17
SK 18
SK 19
SK 20
SK 21
SK 22
SK 23

```

```

C
SUBROUTINE ADD
SUBROUTINE ADD ( NEQ , A , N , B )
DIMENSION A(1) , B(1)
NN = 2*(N-1)
KL = 0
DO 10 J=1,4
DO 10 I=1,J
II = J-I
IJ = NEQ*II+NN+I
KL = KL+1
10 A(IJ) = A(IJ) + B(KL)
RETURN
END

```

```

SA 00
SA 01
SA 02
SA 03
SA 04
SA 05
SA 06
SA 07
SA 08
SA 09
SA 10
SA 11
SA 12

```

```

C
SUBROUTINE SUBM (RO,A1,B1,A2,P2,LENGHT,E*MASS,MASS)
REAL LENGHT, MASS
DIMENSION A(5), W(5), F(4), MASS(10)
DATA A,W / 0., -.538469, .538469, -.906180, .906180, .5633889,
*2*.473629, 2*.236927 /
DO 1 I = 1,10
1 MASS (I) = 0.
DO 2 N = 1,5
X = A(N)
X = .5*(X+1.)
F(3) = X*X*(3.-2.*X)
F(1) = 1.-F(3)
F(2) = X*LENGHT*(1.-2.*X+X*X)
F(4) = X*X*LENGHT*(X-1.)
AA = A1*(1.-X)+A2*X
B = B1*(1.-X)+B2*X
C = 3.14159265*(AA*AA-B*B)*RO*LENGHT/2.*W(N)
E*MASS = E*MASS+C
IJ = 0
DO 2 J = 1,4
DO 2 I = 1,J
IJ = IJ+1
2 MASS (IJ) = MASS(IJ) + C* F(I) * F(J)
RETURN
END

```

```

SM 00
SM 01
SM 03
SM 04
SM 04A
SM 05
SM 06
SM 07
SM 08
SM 09
SM 10
SM 11
SM 12
SM 13
SM 14
SM 15
SM 16
SM 16A
SM 17
SM 18
SM 19
SM 20
SM 21
SM 22
SM 23

```


C
C

```

SUBROUTINE SUBKG (RO, RER, RIB, A1, B1, A2, B2, LENGHT, EMASS, W,
* STIFG)
REAL LENGHT
DIMENSION A(5),W(5),F(4),STIFG(10)
DATA A, W / -.906180, -.538469, 0., .538469, .906180, .236927,
*.478629, .568889, .478629, .236927 /
DM = W / -1
DO 1 I = 1,10
1 STIFG(I) = 0.
DO 2 N = 1,5
X = A(N)
X = .5*(X+1.)
F(1) = X*6.*(X-1.)
F(2) = (1.-4.*X+3.*X*X)*LENGHT
F(3) = -F(1)
F(4) = (3.*X-2.)*LENGHT*X
A3 = (A2-A1)*X + A1
B3 = (B2-B1)*X + B1
QMASS = RO * 3.14159265 * ( DM + X ) * LENGHT / 3. * (( REB * REB
*+ A3*REB + A3*A3 ) - (RIB * RIB + B3*RIB + B3*B3))
P = 9.81 * ( EMASS - QMASS )
IJ = J
DO 2 J = 1,4
DO 2 I = 1,J
IJ = IJ + 1
2 STIFG(IJ) = STIFG(IJ) + P*F(I)*F(J)
RETURN
END

```

SKG 00
SKG 01
SKG 02
SKG 03 *

SKG 05
SKG 06
SKG 07
SKG 08
SKG 09
SKG 10
SKG 11
SKG 12
SKG 13
SKG 14
SKG 15
SKG 16
SKG 17
SKG 18
SKG 19
SKG 20
SKG 21
SKG 22
SKG 23
SKG 25
SKG 26
SKG 27
SKG 28
SKG 29
SKG 30

```

C
C
SUBROUTINE TF (IW,TOWER,NELEM,HIGHT,ZO,RET,REB,DEPTH,
*NEQ,MSW,STIFF,MASS,A,B,FREQ,KQ,NFIGD,H,BETAV,BETAH,ALPHA,
*KD,LENGHT,DA,DB,RIT,S,BETAD,DK,DM,NFREQ,KNW)
COMPLEX A,B,C,G,F,T,R,Q
REAL MASS,LENGHT
DIMENSION TOWER(20),STIFF(1),MASS(1),A(1),B(10),P(4),S(1),US(15),
*VS(15),HS(15),SS(5),FREQ(1),H(1)
J=NELEM+1
DO 100 I=1,J
US(I)=0.0
VS(I)=0.0
HS(I)=0.0
SS(I)=0.0
USD=0.0
HSD=0.0
DO 99 L=1,NFREQ
W=6.29318531*FREQ(L)
W2=W*W
FORM COEFFICIENT MATPIX
LIM = NEQ*MBW
D=W*BETAV+2.*BETAH
G=CMPLX(1.,D)
F=CMPLX(-W2,W*ALPHA)
DO 1 I = 1,LIM
1 A(I)=G*STIFF(I)+F*MASS(I)
IF(KD.EQ.0) GO TO 15
CD=W*2.0*BETAD*SQRT(DK)*SQRT(DM)
T=CMPLX(G.,CD-D*DK)
R=CMPLX(0.,-CD+D*DK)

```

TF 00
TF 01
TF 02

TF 07
TF 08
TF 09

TF 10
TF 12

* * * * *

```

X=D*DK+W*ALPHA*DM
Q=CMPLX(0.,CD-X)
A(NEQ-2)=A(NEQ-2)+T
A(NEQ)=A(NEQ)+Q
A(3*NEQ-2)=A(3*NEQ-2)+R
15 CONTINUE
C
C FORM LOFD VECTOR
DO 2 I = 1,NEQ
2 B(I) = 0.
DN = NELEM
LENGHT = HEIGHT/DN
DA = ( RET-REB)/DN
A1 = REB
DO 4 N = 1,NELEM
A2 = A1 + DA
CALL SUBP (N, A1, A2, LENGHT, Z0, DPTH, W2, P )
J = 2*(N-1)
DO 3 I = 1,4
J = J+1
C=P(I)*H(L)
3 B(J)=B(J)+C
4 A1 = A2
C
C IMPOSE DISPLACEMENT BOUNDARY CONDITIONS
IF(NPIGD.EQ.0) GO TO 9
DO 5 I = 1, LIM, NEQ
A(I) = 0.
5 A(I+1) = 0.
B(1) = 0.
B(2) = 0.
C
C SOLVE SYSTEM OF EQUATIONS

```

```

TF 13
TF 14
TF 15
TF 16
TF 17
TF 19
TF 21
TF 23
TF 24
TF 25
TF 26
TF 27
TF 28
TF 29

```

```

TF 31
TF 32
TF 33
TF 34
TF 35
TF 36
TF 37
TF 38
TF 39
TF 40

```

```

C
C
9 CALL SOLVE (O,IW,NEO,MBW,1,A,P,LIM,NFLEM,RET,RIT,LENGHT,DA,DE,S)
C
C
PRINT OUT STEADY - STATE RESPONSE
IF (KNW.NE.0) GO TO 103
REQ=FFREQ(L)
WRITE(I4,5) TOWER,REQ
103 CONTINUE
I2 = YEQ
IF (KD.EQ.0) GO TO 10
HACC=- (CABS(E(I2))*W2)
Y=CABS(B(I2)-B(I2-2))
USD=USD+Y**2
HSD=HSD+HACC**2
IF (KNW.NE.0) GO TO 101
WRITE(IW,11) Y,HACC
11 FORMAT (13X,E15.5,21X,E15.5)
101 CONTINUE
I2=I2-1
10 CONTINUE
NNODE = NFLEM + 1
DO 7 I = 1,NNODE
J = NNODE-I+1
HACC=- (CABS(B(I2-1))*I2)
U=CABS(B(I2-1))
V=CABS(B(I2))
US(J)=US(J)+U**2
VS(J)=VS(J)+V**2
HS(J)=HS(J)+HACC**2
IF (KNW.NE.0) GO TO 102
WRITE (IW,8) J,U,V,HACC
102 CONTINUE
7 I2 = I2-2
6 FORMAT ('1'/5X,20P4//5X,**STEADY-STATE RESPONSE AT ',F8.3, ' CPS**'
TF 42
TF 43
TF 45
TF 46
TF 47
TF 48
TF 50
TF 51

```

```

*//5X, 'NODE', 6X, 'DISPLACEMENT', 10X, 'ROTATION', 10X, 'ACCELERATION',
*//)
8  FORMAT(5X, I4, 3(3X, E15.5))
   IF (KNW.NE.0) GO TO 104
   WRITE(IW, 12) REQ
104 CONTINUE
12  FORMAT(///5X, '*ELEMENT STRAINS AT ', F8.3, ' CPS*', //5X, 'ELEMENT',
*6X, 'STRAIN'//)
   DO 13 I=1, NEJEM
   SS(I)=SS(I)+S(I)**2
   IF (KNW.NE.0) GO TO 105
   WRITE(IW, 14) I, S(I)
14  FORMAT(5X, I4, 3X, E15.5)
105 CONTINUE
13  CONTINUE
99  CONTINUE
C  COMPUTE AND PRINT RESPONSE STANDARD DEVIATIONS
   WRITE(IW, 107)
107 FORMAT('1/5X, 'RESPONSE STANDARD DEVIATIONS'//5X, 'NODE', 6X,
*'DISPLACEMENT', 10X, 'ROTATION', 10X, 'ACCELERATION'//)
   IF (KD.EQ.0) GO TO 108
   USD=SQRT(USD)
   HSD=SQRT(HSD)
   WRITE(IW, 109) USD, HSD
109 FORMAT(5X, 'DAMPER', 2X, E15.5, 21X, E15.5)
108 CONTINUE
   J=NELEM+1
   DO 110 I=1, J
   US(I)=SQRT(US(I))
   VS(I)=SQRT(VS(I))
   HS(I)=SQRT(HS(I))
110 WRITE(IW, 8) I, US(I), VS(I), HS(I)
   WRITE(IW, 111)

```

```
111 FORMAT(////5X, 'STRAIN STANDARD DEVIATIONS'//5X, 'ELEMENT',5Y,  
* 'STRAIN'//)  
DO 112 I=1,NELEM  
SS(I)=SQRT(SS(I))  
112 WRITE(I*,14) I,SS(I)  
RETURN  
END
```

TF 54
TF 55

C C

```
FUNCTION RK
FUNCTION RK (W2,G,DEPTH)
RK = W2/G
IF ( W2 .EQ. 0. ) RETURN
IF ( RK * DEPTH .LT. 10. ) GO TO 8
RK = 10. / DEPTH
RETURN
8 A2 = 0.
DK = ( 2. - RK ) / 10.
10 A1 = A2
B = RK * DEPTH
A2 = W2 - RK * G *DSINH (B) /DCOSH(B)
IF ( A2 .EQ. 0. ) RETURN
RK = RK + DK
IF ( A1/A2 .GE. 0. ) GO TO 10
RK = RK - 1.5 * DK
DK = DK / 2.
12 IF ( DK/RK .LT. 1.E-4 ) RETURN
B = RK * DEPTH
A3 = W2 - RK * G *DSINH(B) /DCOSH(B)
IF ( A3 .EQ. 0. ) RETURN
DK = DK / 2.
IF ( A3 / A1 .GT. 0. ) GO TO 14
RK = RK - DK
A2 = A3
GO TO 12
14 RK = RK + DK
A1 = A3
GO TO 12
END
```

RK 00
RK 01 *
RK 03
RK 04
RK 05
RK 05A
RK 05B
RK 06
RK 07
RK 08
RK 09
RK 10
RK 11
RK 12
RK 13
RK 14
RK 15
RK 16
RK 17
RK 18
RK 19
RK 20
RK 21
RK 22
RK 23
RK 24
RK 25
RK 25
RK 27
RK 28

```
FUNCTION DCOSH (A)  
R =DEXP(A)  
DCOSH = .5*(R+1./R)  
RETURN  
END
```

```
*  
SP 02  
SP 03  
SP 04  
SP 05
```



```
FUNCTION DSINH (A)
  B = DEXP (A)
  DSINH = .5*(B-1./B)
RETURN
END
```

```
*
SP 07
SP 08
SP 09
SP 10
```

```

C
SURROUTINE SUBP ( N, A1, A2, LENGHT, Z0, DEPTH, W2, P)
REAL LENGHT, K
DIMENSION A(5), W(5), P(4)
DATA A, W / 0., -.538469, .538469, -.906180, .906180, .568889,
* 2*.478629, 2*.236927 /
DATA CI, RO, G / 2., 1., 9.81 /
V = RK ( W2, S, DEPTH )

C
DO 1 I = 1, 4
1 P(I) = 0.
Z1 = Z0 + LENGHT * DFLOAT ( N-1 )
C = 3.1415926 * CI * RO * W2 / DSINH ( K * DEPTH )
DO 2 I = 1, 5
X = A(I)
X = .5 * ( X + 1. )
RADIUS = A1 * ( 1.-X ) + A2 * X
Z = Z1 + LENGHT * X
IF ( Z. GT. DEPTH ) RETURN
F = 2 * RADIUS ** 2 * DCOSH ( K * Z ) * W(I) / 2. * LENGHT
H = X * X * ( 3.-2.*X )
P(1) = P(1) + ( 1.-H ) * F
P(2) = P(2) + ( X * LENGHT * ( 1.-2.*X + X * X ) ) * F
P(3) = P(3) + H * F
P(4) = P(4) + X * X * LENGHT * ( X-1. ) * F
2 CONTINUE
RETURN
END

```

```

SP 00
SP 11
SP 13
SP 14
SP 15
SI 16
SP 15A
SP 17
SP 18
SP 13
SP 20
SP 22
SP 23
SP 24
SP 25
SP 26
SP 27
SP 28
SP 29
SP 30
SP 31
SP 32
SP 33
SP 34
SP 35
SP 36
SP 37

```

```

C    C    C    C    C    C    C    C    C    C    C    C    C    C    C    C    C    C    C    C    C    C    C    C
SUBROUTINE SOLVE
SUBROUTINE SOLVE(IO,IW,NEQ,MBW,NLS,A,B,LIM,NELEM,RET,RIT,LENGHT,
*DA,DR,S)
REAL LENGHT
COMPLEX A(1),B(1),C,D
DIMENSION S(1)
* SOLVES SYMMETRIC SYSTEM OF EQUATIONS USING GAUSSIAN REDUCTION *
IO    OPERATION INDICATOR      0 SOLVES SYSTEM A*X=B
            1 REDUCES MATRIX A
            2 REDUCES AND BACKSUBSTITUTES R
NEQ    NUMBER OF EQUATIONS
MBW    MAXIMUM BANDWIDTH
NLS    NUMBER OF SYSTEMS
A      SUARE BANDED SYMMETRIC POSITIVE DEFINITE MATRIX
        STORED AS MONODIMENSIONAL ARRAY   NEQ*MBW
        ELEMENT A(I,J) IS STORED IN A(I+(J-I)*NEQ)
R      RECTANGULAR ARRAY, STORED COLUMNWISE
*****
C    C    C    C    C    C    C    C    C    C    C    C    C    C    C    C    C    C    C    C    C    C    C    C
REDUCTION OF A. ORIGINAL ARRAY IS DESTROYED
IF (IO.EQ.2) GO TO 20
NRD = NEQ-1
DO 13 I = 1,NRD
D = A(I)
IF (CABS(D).EQ.0.) GO TO 18
IJ=I
DO 16 J=2,MBW
IJ=IJ+NEQ
IF (CABS(A(IJ)).EQ.0.) GO TO 16
C=A(IJ)/D
IK=IJ

```

```

SS 00   *
SS 04
SS 05
SS 06
SS 07
SS 08
SS 09
SS 10
SS 11
SS 12
SS 13
SS 14
SS 15
*****
SS 16
SS 17
SS 18
SS 19
SS 20
SS 21
SS 22
SS 24
SS 25
SS 26
SS 28
SS 29   *

```

SS 30
 SS 31
 SS 32
 SS 33
 SS 34
 SS 35
 SS 36
 SS 37
 SS 38
 SS 39
 SS 40
 SS 41
 SS 42
 SS 43
 SS 45
 SS 46
 SS 47
 SS 49
 SS 50
 SS 51
 SS 52
 SS 53
 SS 54
 SS 55
 SS 56
 SS 55A
 SS 57
 SS 58
 SS 59
 SS 60

*

```

JK=I+J-1
DO 14 K=J,MBW
A(JK)=A(JK)-C*A(IK)
IK=IK+NEQ
14 JK=JK+NEQ
16 CONTINUE
18 CONTINUE
IF (IC.EQ.1) RETURN

C C C
REDUCTION OF B. ORIGINAL ARRAY IS DESTROYED

20 NRE=NEQ-1
DO 26 I=1,NRE
D=A(I)
IF (CABS(D).EQ.0.) GO TO 26
IJ=I
DO 24 J=2,MBW
IJ=IJ+NEQ
IF (CABS(A(IJ)).EQ.0.) GO TO 24
C=A(IJ)/D
IK=I
JK=I+J-1
DO 22 K=1,NLS
B(JK)=B(JK)-C*B(IK)
IK=IK+NEQ
22 JK=JK+NEQ
24 CONTINUE
26 CONTINUE

C C C
BACKSUBSTITUTION. RESULTS STORED IN F.

I=NEQ
30 IF (CABS(A(I)).EQ.0.) GO TO 34

```

```

IK=I
DO 32 K=1,NLS
  B(IK)=B(IK)/A(I)
32 IK=IK+NEQ
34 I=I-1
  IF (.I.EQ.0) GO TO 40
  IJ=I
  DO 38 J=2,NBW
    IJ=IJ+NEQ
    IF (CABS(A(IJ)).EQ.0.) GO TO 38
    IK=I
    JK=I+J-1
    DO 36 K=1,NLS
      B(IK)=B(IK)-A(IJ)*B(JK)
      IK=IK+NEQ
      JK=JK+NEQ
36 CONTINUE
38 GO TO 30
C SOLVE FOR STRAINS
40 I=(NELEM+1)*2
  DO 39 K=1,NELEM
    J=NELEM-K+1
    N=K-1
    D=RET+(FLOAT(N)*DA)+(DA/2.0)-RIT-(FLOAT(N)*DR)-(DR/2.0)
    S(J)=CABS((B(I)-B(I-2))*D/(2.0*LENGHT)
    I=I-2
39 CONTINUE
C RETURN
END

```

```

SS 62
SS 63
SS 64
SS 65
SS 66
SS 68
SS 69
SS 70
SS 72
SS 73
SS 75
SS 76
SS 77
SS 78
SS 79
SS 80

```

```

SS 91
SS 92

```

```

C      SUBROUTINE TIME H ( IW , NEQ , MBW , NREQ , NELEM ,
      *RET , REB , HEIGHT , ZO , DEPTH , DT , TIME ,
      *STIFF , MASS , FREQ , A , B , H , PHASE ,
      *DIS , VEL , ACC , R , S , P , Q , KQ , NRIGD )
      IMPLICIT REAL * 8 ( A-H , O-Z )
      REAL*8 MASS , LENGHT
      DIMENSION DIS( 1 ) , VEL ( 1 ) , ACC ( 2 ) , MASS ( 1 ) ,
      *A( 1 ) , P( 1 ) , S( 1 ) , B( 2 ) , FREQ( 1 ) , H( 1 ) , PHASE( 1 ) ,
      *Q( NEQ , NREQ ) , P( 1 )
      NTIME = TIME / DT
      C      FORM MATRIX OF COEFFICIENTS
      C2 = DT * DT / 6.
      LIM = NEQ * MBW
      DO 50 I = 1 , LIM
      50 A( I ) = MASS( I ) + C2 * STIFF( I )
      C      PRESCRIBE FIRST TWO DDF AS ZERO
      C      IF( NRIGD .EQ. 0 ) GO TO 10
      DO 51 I = 1 , LIM , NEQ
      A( I ) = 0.
      51 A( I+1 ) = 0.
      C      TRIANGULARIZE MATRIX
      C      10 CALL SOLVE ( 1 , IW , NEQ , MBW , 1 , A , B )
      C      FORM VECTOR OF APPLIED FORCES
      DO 5 M = 1 , NREQ
      DO 5 N = 1 , NEQ
      5 Q( N , M ) = 0.
      DN = NELEM

```

```

TH 01
TH 02
TH 03
TH 04
MP 16E
TH 06
TH 07
TH 08
TH 09
TH 10
TH 11
TH 12
TH 13
TH 14
TH 15
TH 16
TH 17
TH 18
TH 19
TH 20
TH 21
TH 22
TH 23
TH 24
TH 25
TH 27
TH 28
TH 29
TH 30
TH 31
TH 32

```

TH 33
 TH 34
 TH 35
 TH 36
 TH 37
 TH 38
 TH 39
 TH 40
 TH 41
 TH 42
 TH 43
 TH 44
 TH 45
 TH 46
 TH 47
 TH 48
 TH 49
 TH 50
 TH 51
 TH 52
 TH 53
 TH 54
 TH 55
 TH 56
 TH 57
 TH 58
 TH 59
 TH 60
 TH 61
 TH 62
 TH 63
 TH 64
 TH 65

```

LENGHT = HEIGHT / DN
DA = ( RET - REB ) / DN
DO 7 N = 1, NREQ
A1 = REB
W2 = (5.28318531 * FREQ(N) ) ** 2
DO 7 I = 1, NELEM
A2 = A1 + DA
CALL SUBP ( I , A1 , A2 , LENGHT , ZC , DEPTH , W2 , P )
J = 2 * ( I - 1 )
DO 8 M = 1, 4
J = J + 1
8 Q( J , N ) = Q( J , N ) + P(M) * H(N)
7 A1 = A2

C
C INITIALIZE DISPLACEMENTS, VELOCITIES, AND ACCELERATIONS
DO 52 I = 1, NEQ
DIS ( I ) = 0.
VEL ( I ) = 0.
52 ACC ( I ) = 0.
TIME = 0.

C
C1 = DT / 2.
C2 = DT * DT / 3.
C3 = C2 / 2.

C
C TIME INTEGRATION (LINEAR ACCELERATION METHOD). NO DAMPING
DO 62 N = 1, NTIME
TIME = TIME + DT

C
DO 9 I = 1, NEQ
9 B(I) = 0.

C
DO 11 J = 1, NREQ
  
```

N

```

C =DCOS ( 6.23318531 * FREQ(J) * TIME - PHASE(J) )
DO 11 I = 1,NEQ
11 R(I) = R(I) + C * Q( I,J )
C
DO 55 I = 1,NEQ
R(I) = VEL(I) + C1 * ACC(I)
S(I) = DIS(I) + DT * VEL(I) + C2 * ACC(I)
55 ACC(I) = R(I)
C
CALL AMBC (NEQ, MBW, ACC, STIFF, S)
IF(NRIGD.EQ.0) GO TO 70
ACC(1) = 0.
ACC(2) = 0.
70 CALL SOLVE ( 2, IW, NEQ, MBW, 1, A, ACC)
C
DO 56 I = 1,NEQ
VEL (I) = R(I) + C1 * ACC(I)
56 DIS(I) = S(I) + C3 * ACC(I)
C
IF(N/50*50-N.NE.0) GO TO 52
WRITE ( IW, 2)      TIME
DO 60 I = 1,NEQ
60 WRITE (IW, 3)  I, R(I), ACC(I), VEL(I), DIS(I)
52 CONTINUE
C
2 FORMAT ( //5X , ' TIME =', F8.2// , 9X , 'I', 8X ,
*'FORCE', 8X , 'ACCELERATION', 6X , 'VELOCITY', 5X ,
*'DISPLACEMENT'// )
3 FORMAT ( 6X , I4 , 4E16.4 )
RETURN
END

```

```

TH 66
TH 67
TH 68
TH 69
TH 70
TH 71
TH 72
TH 73
TH 74
TH 75
TH 76
TH 77
TH 78
TH 79
TH 80
TH 81
TH 82
TH 83
TH 84
TH 85
TH 86
TH 87
TH 88
TH 89
TH 90
TH 91
TH 92
TH 93
TH 94
TH 95
TH 96

```



```

C
SUBROUTINE AMBC (NEQ, MBW, A, R, C )
SUBROUTINE AMBC (NEQ, MBW, A, R, C )
IMPLICIT REAL * 8 ( A-H, O-Z )
DIMENSION A(1), B(1), C(1)
LIM = MPW - 1
DO 1 J = 1, NEQ
A(I) = A(I) - B(I) * C(I)
M = I
DO 7 J = 1, LIM
K = I + J
M = M + NEQ
IF ( K .LE. NEQ ) A(I) = A(I) - B(J) * C(K)
K = I - J
L = M - J
IF ( K .GT. 0 ) A(I) = A(I) - B(L) * C(K)
7 CONTINUE
1 RETURN
END

```

```

AM 00
AM 01
AM 01A
AM 02
AM 03
AM 04
AM 05
AM 06
AM 08
AM 09
AM 10
AM 11
AM 12
AM 13
AM 14
AM 15
AM 16

```

APPENDIX B
MODEL MATRICES

1.0	0	0	0	0	0	0	0	0	0	0	0	0	0	0	0	0	0	0	0
1.0	0	0	0	0	0	0	0	0	0	0	0	0	0	0	0	0	0	0	0
2959.	-3831.	433.6	-9678.	0	0	0	0	0	0	0	0	0	0	0	0	0	0	0	0
6.364E5	9422.	-2016E5	-3334	293.	-6564.	0	0	0	0	0	0	0	0	0	0	0	0	0	0
4.491E5	6344.	1335.	-2839.	173.4	-3911.	0	0	0	0	0	0	0	0	0	0	0	0	0	0
2.877E5	3726.	4598.	-5733.	2.532E6	0	0	0	0	0	0	0	0	0	0	0	0	0	0	0

S
Y
M
M
E
T
R
I
C

Figure B-1
Mass Matrix for 1000 Foot Tower

1.0	0	0	0	0	0	0	0	0	0	0	0	0	0	0	0	0	0	0
1.0	0	0	0	0	0	0	0	0	0	0	0	0	0	0	0	0	0	0
6.23E6	-6.83E7	-1.99E6	7.85E7	0	0	0	0	0	0	0	0	0	0	0	0	0	0	0
1.65E10	-1.04E8	2.76E6	-3.70E7	7.09E9	-4.15E7	1.09E9	0	0	0	0	0	0	0	0	0	0	0	0

S Y M M E T R I C

Figure B-2

Stiffness Matrix for 1000 Foot Tower

1.0	0	0	0	0	0	0	0	0	0	0	0	0	0	0	0	0	0	0	0	0	0
1.0	0	0	0	0	0	0	0	0	0	0	0	0	0	0	0	0	0	0	0	0	0
	2.69E4	-2.94E5	-8.54E3	3.38E5	0	0	0	0	0	0	0	0	0	0	0	0	0	0	0	0	0
		7.10E7	-4.47E5	1.20E7	0	0	0	0	0	0	0	0	0	0	0	0	0	0	0	0	0
			1.19E4	-1.59E5	-3.31E3	1.25E5	0	0	0	0	0	0	0	0	0	0	0	0	0	0	0
				3.05E7	-1.78E5	4.69E6	0	0	0	0	0	0	0	0	0	0	0	0	0	0	0
					4.28E3	-7.23E4	-9.15E2	3.15E4													
						1.02E7	-5.23E4	1.31E6													
							1.06E3	-3.18E4													
								1.66E6													

117

S Y M M E T R I C

Figure B-3

C_1 , Viscous Damping Matrix for 1000 Foot Tower

1.0	0	0	0	0	0	0	0	0	0	0	0	0	0	0	0	0	0	0	0	0
1.0	0	0	0	0	0	0	0	0	0	0	0	0	0	0	0	0	0	0	0	0
	11.87E5	-12.05E6	-15.97E4	12.36E6	18.40E7	18.40E7	0	0	0	0	0	0	0	0	0	0	0	0	0	0
	14.95E8	-13.12E6	18.28E4	-11.11E6	-12.31E4	18.70E5	0	0	0	0	0	0	0	0	0	0	0	0	0	0
				12.13E8	-11.24E6	13.27E7	0	0	0	0	0	0	0	0	0	0	0	0	0	0
				12.95E4	-15.04E5	-6.42E3	12.21E5													
				17.11E7	-13.66E5	19.18E6														
				16.42E3	-12.21E5	11.10E7														

S
Y
M
M
E
T
R
I
C

Figure B-4

C_2 , Hysteretic Damping Matrix for 1000 Foot Tower

1.0	0	0	0	0	0	0	0	0	0
1.0	0	0	0	0	0	0	0	0	0
4009.	-6455.	581.	-1.514E4	0	0	0	0	0	0
1.174E6	1.471E4	-3.675E5	0	0	0	0	0	0	0
2757.	-5545.	380.	-9954.	0	0	0	0	0	0
8.079E5	9591.	1695.	-2.407E5	0	0	0	0	-5622.	-1.348E5
4.956E5	-4630.	213.	5324.	8001.	-8091.	2.597E6			

S Y M M E T R I C

Figure B-5

Mass Matrix for 1200 Foot Tower

1.0	0	0	0	0	0	0	0	0	0	0	0	0	0	0	0	0	0	0	0
	1.0	0	0	0	0	0	0	0	0	0	0	0	0	0	0	0	0	0	0
		5.69E6	-7.63E7	-1.77E6	8.06E7	0	0	0	0	0	0	0	0	0	0	0	0	0	0
			2.03E10	-1.08E8	3.39E9	0	0	0	0	0	0	0	0	0	0	0	0	0	0
				2.41E6	-3.98E7	-6.43E5	2.78E7	0	0	0	0	0	0	0	0	0	0	0	0
					8.32E9	-4.07E7	1.24E9	0	0	0	0	0	0	0	0	0	0	0	0
						8.02E5	-1.70E7	-1.60E5	6.21E6										
							2.56E9	-1.08E7	3.12E8										
								1.60E5	-6.21E6										
										1.60E5									
																			3.51E8

S
Y
M
M
E
T
R
I
C

Figure B-6

Stiffness Matrix for 1200 Foot Tower


```
1.0  0  0  0  0  0  0  0  0  0  0  0  0  0  0  0  0  0
      1.0  0  0  0  0  0  0  0  0  0  0  0  0  0  0  0  0  0
      3.37E4  -4.50E5  -1.04E4  4.75E5  0  0  0  0  0  0  0  0  0  0  0
      1.20E8  -6.37E5  -6.37E5  2.00E7  -2.35E5  -3.78E3  1.64E5  0  0  0  0  0
      1.43E4  -2.91E7  -2.40E5  4.91E7  -2.40E5  7.31E6  0  0  0  0  0  0
      4.77E3  -1.00E5  -9.39E2  3.65E4
      1.51E7  -6.36E4  1.84E6
      1.60E5  -3.68E4
      2.13E6
```

```
S Y M M E T R I C
```

Figure B-7

\underline{C}_I , Viscous Damping Matrix for 1200 Foot Tower

1.0	0	0	0	0	0	0	0	0	0	0	0	0	0	0	0
	0	0	0	0	0	0	0	0	0	0	0	0	0	0	0
	11.71E5	-12.29E6	-15.31E4	12.42E5	0	0	0	0	0	0	0	0	0	0	0
	16.09E8	-13.24E6	-17.23E4	11.02E8	-11.19E6	-11.93E4	18.34E5	0	0	0	0	0	0	0	0
			17.23E4	-11.19E6	-11.93E4	18.34E5	0	0	0	0	0	0	0	0	0
				12.50E8	-11.22E6	-11.72E7	13.72E7	0	0	0	0	0	0	0	0
					12.41E4	-15.10E5	-14.80E3	11.86E5							
					17.68E7	-13.24E5	19.36E6								
					14.80E3	-11.87E5	11.05E7								

S
Y
M
M
E
T
R
I
C

Figure B-8
 \underline{C}_2 , Hysteretic Damping Matrix For 1200 Foot Tower

1.522E4	4.592E5	32.	-342.	0	0	0	0	0	0	0	0	0	0	0	0	0	0	0
	1.532E6	331.	-3361.	0	0	0	0	0	0	0	0	0	0	0	0	0	0	0
		148.	-143.	19.	-208.	0	0	0	0	0	0	0	0	0	0	0	0	0
			7147.	198.	-2035.	0	0	0	0	0	0	0	0	0	0	0	0	0
				83.	-108.	10.	-107.	0	0	0	0	0	0	0	0	0	0	0
					4044.	100.	-1034.	0	0	0	0	0	0	0	0	0	0	0
						37.	-73.	3.	-38.									
							1809.	34.	-359.									
								1586.	-46.									
																		5.006E5

S Y M M E T R I C

Figure B-9

Mass Matrix for Condeep

6.87E6	2.11E8	-5.68E6	1.06E8	0	0	0	0	0	0	0	0	0
9.77E9		-1.39E8	1.78E9	0	0	0	0	0	0	0	0	0
	7.96E6		-4.88E7	-2.28E6	4.10E7	0	0	0	0	0	0	0
		4.58E9		-5.75E7	7.19E8	0	0	0	0	0	0	0
			2.98E6	-2.26E7	-6.98E5	1.18E7	0	0	0	0	0	0
				1.63E9	-1.84E7	2.23E8	0	0	0	0	0	0
					8.28E5	-8.04E6	-1.31E5	1.92E6				
						4.04E8	-3.71E6	4.27E7				
							1.31E5	-1.92E6				
												4.04E7

S Y M M E T R I C

Figure B-10
Stiffness Matrix for Condeep

3.36E4	1.03E5	-2.81E4	5.09E5	0	0	0	0	0	0	0
	4.20E7	-6.67E5	8.54E6	0	0	0	0	0	0	0
		3.92E4	-2.34E5	-1.09E5	1.97E5	0	0	0	0	0
			2.20E7	-2.76E5	3.45E6	0	0	0	0	0
				1.43E4	-1.08E5	-3.35E3	5.66E4	0	0	0
					1.82E6	-8.83E4	1.07E6	0	0	0
						3.98E3	-3.86E4	-6.29E2	9.21E3	
							1.94E6	-1.78E4	2.05E5	
								6.95E2	-9.22E3	
									2.15E5	

S Y M M E T R I C

Figure B-11

\underline{C}_1 , Viscous Damping Matrix for Condeep

i2.06E5	i6.33E6	-i1.76E5	i3.18E6	0	0	0	0	0	0	0	0	0	0	0	0	0	0	0	0	0
i2.93E8		-i4.17E6	i5.34E7	0	0	0	0	0	0	0	0	0	0	0	0	0	0	0	0	0
	i2.39E5		-i1.46E6	-i6.84E4	i1.23E6	0	0	0	0	0	0	0	0	0	0	0	0	0	0	0
		i1.37E8	i1.72E6	i1.72E6	i2.16E7	0	0	0	0	0	0	0	0	0	0	0	0	0	0	0
			i8.94E4	-i6.78E5	-i2.09E4	i3.54E5	0	0	0	0	0	0	0	0	0	0	0	0	0	0
			i4.89E7	-i5.53E5	i6.67E6	0	0	0	0	0	0	0	0	0	0	0	0	0	0	0
			i2.48E4	-i2.41E5	-i3.93E3	i5.76E4														
			i1.21E7	-i1.11E5	i1.21E6															
			i3.95E3	-i5.76E4																
			i1.21E6																	

S Y M M E T R I C

Figure B-12

C_2 , Hysteretic Damping Matrix for Condeep

APPENDIX C

MODAL ANALYSIS OF THE WAVE EXCITED PLATFORM

It is a characteristic of mechanical systems that a normal mode exists for each degree of freedom. Associated with each normal mode is a natural frequency and a characteristic shape. A normal mode is distinguished by the fact that the system, when properly excited, could vibrate freely in that mode alone. When this occurs the ratio of the displacements of any two degrees of freedom is constant with time. These ratios define the characteristic shape of the mode. Most important, the complete motion of the system may be obtained by superimposing the independent motions of the individual modes.

By examining the motion in the normal modes and the contribution of each mode to the total motion of the excited system, it is possible to determine the nature of the motion in terms of how much each mode participates in the total motion.

The modal analysis will be carried out on the 1000 foot platform used as an example in Chapter 3. It will be excited by the same 100 year return sea state discretized into twenty-five frequencies.

C.1 Natural Frequencies and Characteristic Shapes [23]

The equations of motion for an undamped multi-degree of freedom system may be written as

$$\underline{M} \ddot{\underline{x}} + \underline{K} \underline{x} = \underline{F} \quad (C.1)$$

where \underline{M} and \underline{K} are symmetric.

If the system is vibrating in a normal mode, which must be harmonic with time, then:

$$\underline{x} = \underline{X}_n \sin \omega t$$
$$\ddot{\underline{x}} - -\omega_n^2 \underline{X}_n \sin \omega t \quad (C.2)$$

$$\underline{p} = 0$$

Substituting these equations into the equation of motion yields:

$$-\omega_n^2 \underline{M} \underline{X}_n + \underline{K} \underline{X}_n = 0$$

or

$$(\underline{K} - \omega_n^2 \underline{M}) \underline{X}_n = 0 \quad (C.3)$$

where \underline{X}_n is the vector of modal displacements for the n^{th} mode.

Since \underline{X}_n can not be zero, then $(\underline{K} - \omega_n^2 \underline{M}) = 0$ which by Cramer's Rule becomes

$$|\underline{K} - \omega_n^2 \underline{M}| = 0 \quad (C.4)$$

This is a characteristic value problem and the roots of Equation (C.4) are the characteristic numbers, or eigenvalues, which are equal to the squares of the natural frequencies of the modes.

For each root there is a characteristic vector solution \underline{X}_n having an arbitrary magnitude and representing the characteristic shape of that mode.

There are various schemes for solving the characteristic value problem above and there is normally one available as a program

package at any computer facility. The one used for this work was Access II, available at the Joint Computer Facility, M.I.T.

The vectors \underline{X}_n are arranged as columns of the matrix $\underline{\Phi}$, the modal matrix of the system, such that:

$$\underline{\Phi} = [\{\underline{X}_1\}\{\underline{X}_2\}\dots\{\underline{X}_n\}]$$

C.2 Orthogonality of Modes

The orthogonality condition which will be established in this section is important to the development of the modal equations. For any two roots corresponding to the n^{th} and m^{th} modes, Equation C.3 is

$$\omega_n^2 \underline{M} \underline{X}_n = \underline{K} \underline{X}_n \quad (\text{C.5a})$$

$$\omega_m^2 \underline{M} \underline{X}_m = \underline{K} \underline{X}_m \quad (\text{C.5b})$$

Postmultiply the transpose of (C.5a) by \underline{X}_m , thus

$$(\omega_n^2 \underline{M} \underline{X}_n)^T \underline{X}_m = (\underline{K} \underline{X}_n)^T \underline{X}_m$$

or

$$\omega_n^2 \underline{X}_n^T \underline{M}^T = \underline{X}_n^T \underline{K}^T \underline{X}_m \quad (\text{C.6})$$

Premultiply Equation (C.5b) by \underline{X}_n^T , thus

$$\omega_m^2 \underline{X}_n^T \underline{M} \underline{X}_m = \underline{X}_n^T \underline{K} \underline{X}_m \quad (\text{C.7})$$

Since $\underline{M}^T = \underline{M}$ and $\underline{K}^T = \underline{K}$ because both are symmetric, then the right

hand sides of Equations (C.6) and (C.7) are equal. Subtracting Equation (C.7) from Equation (C.6) yields

$$(\omega_n^2 - \omega_m^2) \underline{X}_n^T \underline{M} \underline{X}_m = 0 \quad (C.8)$$

Since $\omega_n^2 \neq \omega_m^2$

$$\underline{X}_n^T \underline{M} \underline{X}_m = 0$$

which is the orthogonality condition. From Equation (C.6) it can also be seen that

$$\underline{X}_n^T \underline{K} \underline{X}_m = 0$$

C.3 Modal Equations

Starting with the system equation of motion:

$$\underline{M} \ddot{\underline{x}} + \underline{K} \underline{x} = \underline{P} \quad (C.1)$$

Let $\underline{x} = \underline{\Phi} \underline{u}$, where \underline{u} is the vector of modal amplitudes. This states that the displacement vector \underline{x} is a linear combination of modal values. Substitution into the equation of motion yields:

$$\underline{M} \underline{\Phi} \ddot{\underline{u}} + \underline{K} \underline{\Phi} \underline{u} = \underline{P} \quad (C.9)$$

Premultiply by $\underline{\Phi}^T$:

$$\underline{\Phi}^T \underline{M} \underline{\Phi} \ddot{\underline{u}} + \underline{\Phi}^T \underline{K} \underline{\Phi} \underline{u} = \underline{\Phi}^T \underline{P} \quad (C.10)$$

Consider $\underline{\Phi}^T \underline{M} \underline{\Phi}$. Each element in the resultant matrix equals

$$M_{ij} = \underline{X}_i^T \underline{M} \underline{X}_j$$

This equals zero for all $i \neq j$ because of orthogonality. Therefore the resultant matrix is a diagonal matrix called the equivalent mass matrix \underline{M}_e whose elements are:

$$M_i = \underline{X}_i^T \underline{M} \underline{X}_i$$

The same result is obtained from $\underline{\Phi}^T \underline{K} \underline{\Phi}$ which becomes \underline{K}_e whose elements are

$$K_i = \underline{X}_i^T \underline{K} \underline{X}_i$$

Returning to Equation (C.10) which is now

$$\underline{M}_e \ddot{\underline{u}} + \underline{K}_e \underline{u} = \underline{\Phi}^T \underline{P}$$

This is a series of n uncoupled differential equations

$$M_1 \ddot{u}_1 + K_1 u_1 = (\underline{\Phi}^T \underline{P})_1$$

$$M_2 \ddot{u}_2 + K_2 u_2 = (\underline{\Phi}^T \underline{P})_2$$

$$\vdots$$

$$M_n \ddot{u}_n + K_n u_n = (\underline{\Phi}^T \underline{P})_n$$

which can be solved individually such that

$$u_i = \frac{(\underline{\Phi}^T \underline{P})_i}{K_i - M_i \omega^2} \sin \omega t + A_i \sin\left(\sqrt{\frac{K_i}{m_i}} t + \theta_i\right) \quad (C.11)$$

where u_i is the sum of the forced and free modal responses.

Up to this point damping has been ignored in the analysis.

If damping had been included, the original equation of motion would

have been

$$\underline{M} \ddot{\underline{x}} + \underline{K} \underline{x} + \underline{C} \dot{\underline{x}} = \underline{P}$$

Carrying out the same analysis as above and ignoring the free vibration portion of the solution; then

$$u_i = \frac{(\underline{\Phi}^T \underline{P})_i}{\sqrt{(K_i - M_i \omega^2)^2 + c_i^2 \omega^2}} \quad (C.12)$$

Critical damping, c_c , is defined as the damping which eliminates any harmonic vibration and is equal to $2\sqrt{KM}$ for a one degree of freedom system.

The ratio of damping to critical damping is the percent of damping in the system, which is labeled p .

Therefore

$$p = \frac{c}{c_c} = \frac{c}{2\sqrt{KM}}$$

Then

$$c = (p)(2\sqrt{KM})$$

Substituting for c in Equation (C.12) yields

$$u_i = \frac{(\underline{\Phi}^T \underline{P})_i}{\sqrt{(K_i - M_i \omega^2)^2 + 4p^2 K_i M_i \omega^2}}$$

As was pointed out in Chapter 2, damping in the computer model was of two types which varied with each frequency and therefore with each mode. For simplification, damping will be assumed to be a

total of 3% of critical damping in all modes for this modal analysis. This is conservative for this procedure because it will tend to reduce the suppression of higher modes which occurs in real structures.

The point has been reached where n steady-state solutions for u_i exist where u_i includes damping. The \underline{u} vector has been formed.

Recalling that $\underline{x} = \underline{\phi} \underline{u}$ the solution for \underline{x} in terms of modal participation has been reached where

$$\begin{aligned} x_1 &= \phi_{11}u_1 + \phi_{12}u_2 + \dots + \phi_{1n}u_n \\ x_2 &= \phi_{21}u_1 + \phi_{22}u_2 + \dots + \phi_{2n}u_n \\ &\vdots \\ x_n &= \phi_{n1}u_1 + \phi_{n2}u_2 + \dots + \phi_{nn}u_n \end{aligned}$$

The displacement of each degree of freedom is expressed as a linear combination of modal displacements. The percentage contribution of any mode to the displacement of any degree of freedom can be found by

% contribution of i th node to j th DOF =

$$\frac{|\phi_{ji}u_i|}{|\phi_{j1}u_1| + |\phi_{j2}u_2| + \dots + |\phi_{jn}u_n|} \quad (C.13)$$

The above discussion is concerned with only one input \underline{P} . In the analysis of a tower subject to excitation by a wave spectrum which has been discretized into N frequencies, the input vector \underline{P} becomes a function of frequency. Evaluating the modal solution at

each frequency yields N modal solutions. To find the rms value of the total response of each degree of freedom the solution of each degree of freedom at each frequency was used in the following formula

$$(\sigma_x)_i = \sqrt{\sum_{j=1}^N (x_i)_j^2} \quad (C.14)$$

where

i = ith DOF

j = jth frequency

If the same formula is used to evaluate the contribution of each mode to the rms value of the total response of each degree of freedom, the result is

$$(\sigma_x)_i = \sqrt{\sum_{j=1}^N [(\underline{\phi} \underline{u})_i]_j^2} \quad (C.15)$$

where

i = ith DOF

j = jth frequency

When the term $(\underline{\phi} \underline{u})_i$ is squared the separation of each modal contribution is lost and the solution $(\sigma_x)_i$ cannot be found in terms of modal contribution.

In order to evaluate the modal contribution to the rms value of the response, the following procedures are used.

At each frequency j, solve the equation of motion

$$\frac{M}{e} \ddot{u}_j + \frac{K}{e} u_j = \frac{\phi^T P}{-j} \quad j = 1, N$$

with

$$u_{ji} = \frac{(\frac{\phi^T P}{-j})_i}{\sqrt{(K_i - M_i \omega_j^2)^2 + 4p^2 K_i M_i \omega_j^2}} \quad \begin{matrix} j=1, N \\ i=1, M(\text{number of modes}) \end{matrix}$$

so that

$$\underline{x}_j = \underline{\phi} \underline{u}_j$$

Procedure A

At each frequency j evaluate the contribution of each mode to the total response. Then sum the contributions of the mode of interest for all frequencies $j = 1, N$ and find the average contribution of that mode.

Procedure B

Assuming that the sum of contributions to the total response of all higher modes at any frequency is small compared to the contribution of the first mode at that frequency, evaluate the following formula

% Contribution of first mode to RMS value of total response for DOF $i =$

$$\frac{\sqrt{\sum_{j=1}^N (\phi_{i1} u_{1j})^2}}{\sqrt{\sum_{j=1}^N [\sum_{K=1}^N |\phi_{iK} u_{Kj}|]^2}} \times 100 \quad (C.16)$$

This formula states that the percent contribution of the first mode to the numerical sum of the modal components for a particular degree of freedom equals the square root of the sum of the squares of the first mode contribution at that DOF for each frequency divided by the square root of the sum of the squares of the numerical sum of the modal components at that DOF for each frequency times 100.

After the results of these two procedures are obtained, chose the most conservative figure for evaluation.

C.4 Platform Analysis and Results

The mass and stiffness matrices for the tower were obtained and the natural frequencies and modal matrix $\underline{\Phi}$ were determined. The next step is to evaluate the equivalent mass and stiffness matrices where

$$\underline{M}_e = \underline{\Phi}^T \underline{M} \underline{\Phi}$$

$$\underline{K}_e = \underline{\Phi}^T \underline{K} \underline{\Phi}$$

The input vectors \underline{P} were obtained for each of twenty-five frequencies in the discretized wave spectrum by evaluation of the work equivalent forces by DuVall's finite element program.

At each frequency the vector $\underline{\Phi}^T \underline{P}$ was evaluated and the vector of modal amplitudes \underline{u} was evaluated. The percent modal contribution will be evaluated for the deck displacement which is DOF number 9 or x_7 . Evaluating $\underline{x} = \underline{\Phi} \underline{u}$ at each frequency and examining x_7 yields the following results.

Table C.1 shows that the first mode varies for percent contribution to the total response from a low of 96.0% to a high of 99.8%. The second mode generally provides the remainder of the response but only 3.0% at the highest.

Using Procedure A and averaging the first mode contribution the result shows the first mode participates in the response with an average of 98.3%.

Using Procedure B and evaluating Equation C.16 yields

$$\frac{\sqrt{\sum_{j=1}^{25} (\phi_{71} u_{1j})^2}}{\sqrt{\sum_{j=1}^{25} \left[\sum_{K=1}^8 |\phi_{7K} u_{Kj}| \right]^2}} \times 100 = 99.2\%$$

The most conservative of these results indicates that the response is that of a one degree of freedom system and that contributions from higher modes can be ignored.

Two other factors must be considered. First, how does the modal participation change if the sea state is less intense, causing the distribution of wave heights versus frequency in the sea spectrum to shift. Secondly, how does the modal participation change if the structure is much stiffer, placing the fundamental frequency of the structure in the range of frequencies where the sea spectrum is more level. This results in all the higher modes being excited by waves of nearly equal intensity.

Malhotra and Penzien [24] did a study which answers the

Freq.	% Mode 1	% Mode 2	$(\phi_{71}u_1)^2$	$(\sum_{K=1}^n \phi_{7K}u_K)^2$
.03	96.6	2.7	3.96E-2	4.24E-2
.042	96.0	2.4	6.02E-1	6.54E-1
.046	97.1	2.4	5.68E-1	6.02E-1
.5	97.3	2.3	6.45E-1	6.82E-1
.054	97.4	2.2	7.79E-1	8.21E-1
.06	97.5	2.1	7.35E-1	7.72E-1
.066	97.7	2.0	5.72E-1	5.99E-1
.072	96.5	1.8	3.92E-1	4.21E-1
.078	97.0	1.8	3.60E-1	3.75E-1
.09	98.2	1.6	2.14E-1	2.22E-1
.102	98.3	1.5	2.26E-1	2.34E-1
.114	98.5	1.3	2.47E-1	2.55E-1
.126	98.7	1.2	2.96E-1	3.05E-1
.138	98.8	1.0	3.71E-1	3.80E-1
.15	99.0	.8	7.02E-1	7.15E-1
.175	99.5	.4	3.06	3.09
.186	99.7	.2	4.37	4.39
.192	99.8	.2	4.78	4.80
.196	99.8	.2	3.90	3.92
.2	99.8	.2	2.47	2.48
.204	99.7	.3	1.36	1.37
.208	99.6	.3	1.85	1.87
.275	99.2	.7	8.24E-1	8.38E-1
.25	98.4	1.4	3.51E-1	3.62E-1
.3	96.6	3.0	1.26E-1	1.34E-1

Table C.1

Response Statistics of DOF 9 (x_7) of 1000 Foot Tower

• first question. They showed that varying the input sea states from one based on a wind speed of 60 miles per hour ($H_s = 36$ feet) to one based on a wind speed of 30 miles per hour ($H_s = 9$ feet) reduced the participation of the first mode only 3%. When the sea state was reduced below those based on a wind speed of 30 miles per hour, the decrease in first mode participation became more pronounced, but the total response in these seas is negligible.

The second question was tackled by Millman [25] in his analysis of an offshore platform with a fundamental frequency of .754 cycles per second ($T = 1.3$ seconds). His modal analysis of this structure excited by a strong sea state ($H_s = 38$ feet) showed the first mode participation in the total response to be on the order of 97%, clearly still dominant.

The result is that independent of sea state or fundamental frequency of this type of tower, the first mode participation in the total response should not fall out of the extremely dominant range.

There are two conclusions which can be drawn from this result. First that higher modes can be ignored when considering methods of reducing the dynamic response of the tower and second that results obtained by DenHartog and Crandall and Mark in their work with vibration absorbers on one degree of freedom systems should be applicable to the mass damper applied to this tower.

Therefore the mass damper should be effective and it should be tuned to suppress the response of the first mode.